THESIS

APPLICATION OF STRUCTURAL HEALTH MONITORING FOR DAMAGE IDENTIFICATION IN AN INDUSTRIAL FAN ROTOR USING IN-SITU MODAL ANALYSIS TESTING

Submitted by

Chad M. Wilcox

Department of Mechanical Engineering

In partial fulfillment of the requirements

For the Degree of Master of Science

Colorado State University

Fort Collins, Colorado

Summer 2014

Master's Committee:

Advisor: Bryan D. Willson

David G. Alciatore
Bogusz J. Bienkiewicz

ABSTRACT

APPLICATION OF STRUCTURAL HEALTH MONITORING FOR DAMAGE IDENTIFICATION IN AN INDUSTRIAL FAN ROTOR USING IN-SITU MODAL ANALYSIS TESTING

A testing procedure is desired which can be applied in manufacturing environments to determine the structural integrity of rotating components within a machine. Current non-destructive evaluation (NDE) of components includes visual inspection, dye penetrant, and x-ray testing. Each of these NDE techniques have limitations in manufacturing plants given very limited time frames and access to rotating components. Vibration condition monitoring is widely used and accepted as a beneficial way to determine faults in rotating equipment. Current vibration condition monitoring practices rely on measurement and analysis of response data. The response data is affected by both changing forces and structural parameters of the system being measured. Therefore, determining whether forces have changed or the structure has been compromised is not readily determined from vibration condition monitoring data.

Structural health monitoring (SHM) has been implemented for a variety of structural faults including: cracking and breaking, loosening of assembled parts, flaws and voids caused by manufacturing, and improper assembly of parts (Wolff & Richardson, 1989). Many studies in the area of SHM have focused on idealized test setups and have used only simulated data. This study focuses on implementation of SHM on the rotating assembly of an industrial fan. The data and results from SHM are used to validate whether or not the structure has been compromised.

TABLE OF CONTENTS

Abstract ii

Introduction 1

Background 4

Theoretical Approach 7

Experimental Approach 12

Experimental Procedures 14

In-situ Testing Setup 14

Lab Testing Setup 16

Instrumentation 21

Detailed Experimental Procedure 23

Data Processing 29

Analysis Procedures 30

Results 33

Global Data Comparisons 33

Case #1: As Built Compared to Bolt 10 Removed 33

Case #2: Bolt 10 and 2, 40 ft-lb Compared to Bolt 2 Removed 35

Case #3: As Built Compared to Bolt 10 and 2, 40 ft-lb 37

Case #4: Bolt 10 Removed Compared to Bolt 2 Removed 40

Local Frequency and Damping 42

Errors and limitation of results 46

Conclusions 53

Bibliography 56

Appendix A 58

Appendix B 63

Instrumentation Specifications 63

Appendix C 64

MAC Data 64

Local Frequency and Damping Comparison 65

Introduction

The use of predictive technologies is widely accepted in manufacturing environments where rotating equipment availability is crucial to the production of goods. Vibration condition monitoring is one of the main predictive technologies utilized in the industry to identify faults in rotating equipment. If these faults go undetected they often lead to unexpected downtime as a result of failed components. The ability to collect data without interfering with production is crucial, making vibration condition monitoring more effective than Non-Destructive Evaluation (NDE) techniques. The presence of increasing or excessive vibration in a machine indicate a fault may be present. Vibration signature analysis is utilized to identify the probable source of the fault. The primary method for measuring vibration signatures of rotating equipment with rolling element bearings is to use accelerometers mounted directly to equipment bearing housings as shown in Figure 1.

Figure 1. Accelerometers mounted to a bearing housing for vibration measurements.

If the vibration signature consists of high vibration at shaft frequency, multiple forces could be contributing to the running speed vibration response vector. Forces include unbalance, misalignment, and others. The vibration response data are not only influenced by the forces acting on the system but are also are affected by the structural properties mass, stiffness, and damping. Worn components and compromised structures affect the structural properties and therefore will have an influence on the vibration response signature. Analysts must try to determine if changes to response data are a result of varying forces, changing system properties, or a combination of both. Current best practices include utilizing spectral, time waveform, and phase response data to differentiate between faults. These data do not always provide the necessary information to differentiate between changing forces and changing system properties. The result is recommendations are often made on the assumption the force is the root cause for the change in vibration signature. If this assumption is inaccurate maintenance procedures performed to eliminate or reduce the force will not be effective and excessive vibration will still be present. Decisions must then be made to overhaul, replace, or run the equipment at excessive vibration amplitudes without conclusive data to support decisions.

Experimental determination of the system properties of rotating equipment provides the information necessary to differentiate between changes in forces or changes in system properties when applied in conjunction with operating response measurements. Structural health monitoring of the rotating assembly will provide information to determine if damage exists that is changing system properties, primarily stiffness and damping.

Results obtained from this study show compromising a single fastener does not significantly change the natural frequency adequately to use as a structural health monitoring indicator. This supports the theoretical calculations performed for a SDOF system. However, the removal of a fastener does significantly affect damping. The review of data consistency shows limitations to damping resulting from significant deviation in local data. The mounting method used was also found to have a significant influence on damping of the rotor. These results did not produce a simple and quick test procedure for in-situ SHM.

Global data results show significant sensitivity of mode shapes to structural changes. The comparison of mode shapes uses the modal assurance criterion (MAC) between different configurations. MAC does provide data to indicate structural changes occurred within the rotor assembly. These results indicate detailed study that includes mode shapes does provide the information necessary for SHM of the rotating assembly.

Background

Many studies have been performed in the area of structural health monitoring (SHM) producing experimental results using simulated data (Hwang & Kim, 2004) and simplified experimental test setups (Liu, Gurgenci, & Veidt, 2004) (Karthikeyan & Tiwari, 2010). In a literature review of SHM by Los Alamos, the authors highlighted the need for studies to focus on specific applications and utilize actual equipment used in industry to prove the benefits of SHM (Doebling, Farrar, Prime, & Shevitz, 1996). This study applies structural health monitoring using forced response measurements to an industrial fan rotor. The SHM is used to identify a compromised bolted connection within the rotating assembly.

The rotor to be tested is a fan utilized in glass manufacturing plants for mold cooling air to the forming machines. This type of fan is critical to production and has a history of excessive vibration that cannot be reduced by typical precision maintenance actions. Many manufacturing environments, including glass plants, operate twenty-four hours per day and seven days per week with only a few maintenance opportunities per year. The duration of each shutdown is kept to a minimum, typically no more than thirty minutes to an hour. Vibration condition monitoring may not provide conclusive data to determine whether the rotor has defects that necessitate replacement. This specific application needs a testing procedure to determine the structural health of the rotor.

In order for a SHM procedure to be practical in many manufacturing environments it must be able to be completed quickly with limited access to the rotating components. Non-destructive

evaluation (NDE) of components used in industry include: visual inspection, dye penetrant, and x-ray testing. Each of these NDE techniques have limitations in manufacturing plants given very limited time frames and access to rotating components. In cases where time does not permit use of these NDE methods plants either continue to operate the machine subject to excessive vibration, or they overhaul and replace the entire machine. These maintenance decisions are made without the necessary information to make justified, data driven decisions. In a few cases where the decision was made to continue to run the machine, components have failed catastrophically, which lead to ancillary damage and increased downtime.

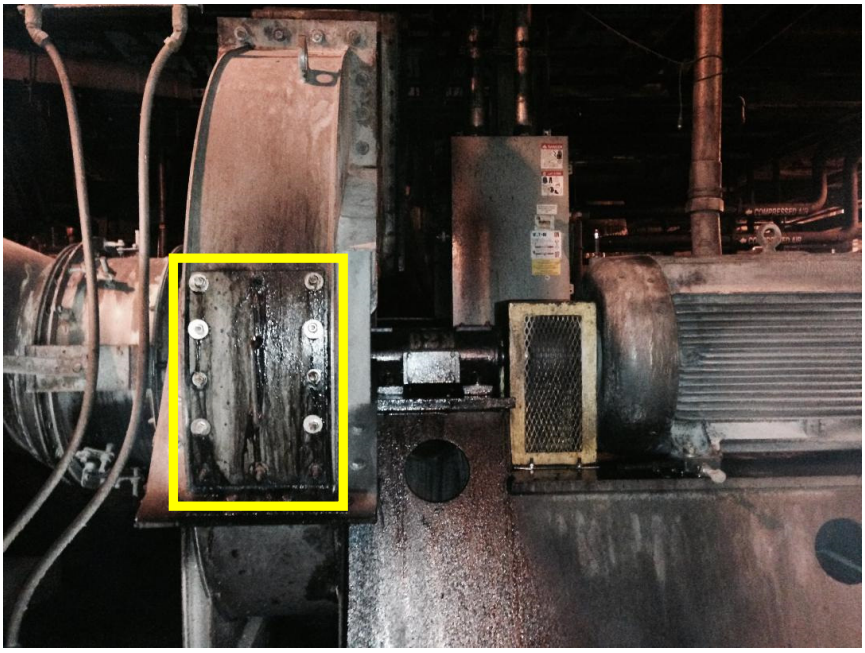

Figure 2. Mold fan at a manufacturing facility.

Figure 2 shows a typical mold cooling fan at a glass manufacturing facility. An inspection door on the side of the fan housing, identified by the yellow square in Figure 2, provides the only access to the rotor. The access door can be removed quickly for test purposes once the machine is shutdown. Given the limited access to the rotor and minimal time available for testing, a test procedure is necessary which would make use of a few collection locations on the fan and a

simple structural excitation. Wolff and Richardson showed that a local change to a structure, such as a removed fastener, will change global modes and can be quantified by modal analysis (Wolff & Richardson, 1989). A change in modal parameters of a global mode affects nearly all collection locations. Therefore, a measurement of just a few collection locations makes it possible to determine a change in natural frequency and damping.

In summary, in-situ forced response measurements of the rotor provide practical means for NDE of the rotor within a typical manufacturing environment. The modal testing can be accomplished in minimal amount of time by collecting a few frequency response functions (FRF's) of the rotor. Use of a modal impact hammer provides the necessary simple means of structure excitation and allow it to be implemented thru the access door of the fan housing.

Theoretical Approach

It is widely accepted and can be shown theoretically that modal parameters (frequency, damping, and mode shapes) change with physical changes to a structure. Many studies have been conducted to illustrate the sensitivity of modal parameters to damage in structures, such as cracks and loose connections between subassemblies. In a study by Wolff and Richardson, natural frequencies changed by as much as 30 Hz on a plate with a rib stiffener by removing a bolt from the end of the rib (Wolff & Richardson, 1989). The results also showed substantial changes to global mode shapes. This study focuses on a compromised bolted connection on the back plate of a fan rotor. A structural change like this is expected to change the natural frequency and damping. The rotor will be subjected to a compromised bolted connection by removing a fastener and altering fastener torque. Figure 3 is a schematic of the fan assembly representing a simplification of the structure to be tested.

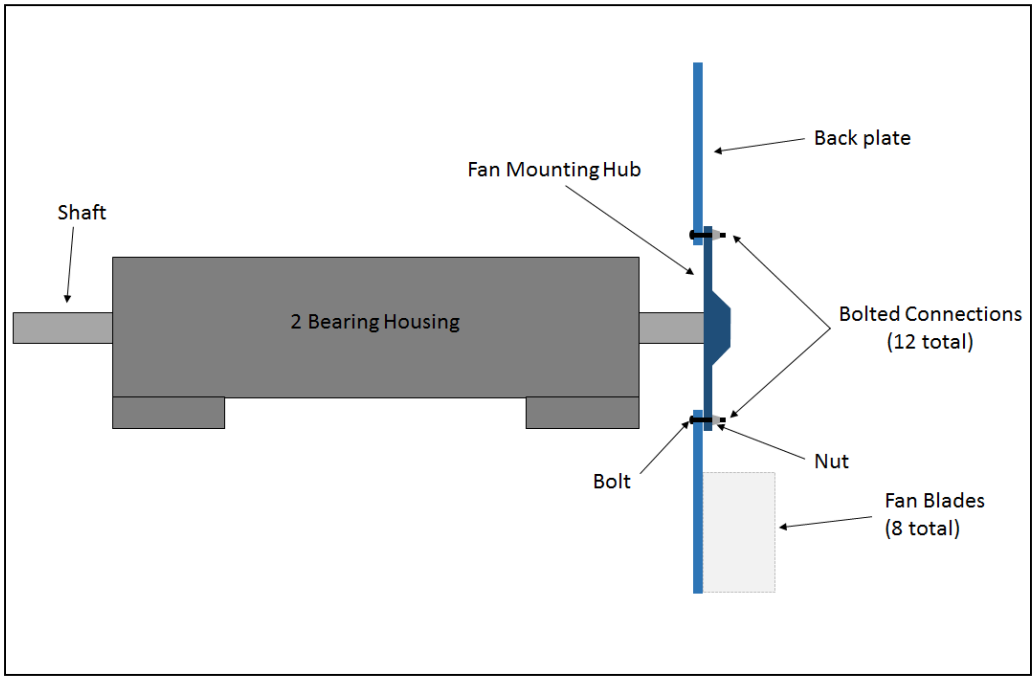

Figure 3. Schematic representing the fan assembly to be tested.

A single degree of freedom (SDOF) representation of the closed form solution is used to model the back plate of the fan. This is completed to investigate if changing stiffness of the bolted connection changes the natural frequency of an undamped SDOF system. The equation of motion for the SDOF spring mass system is shown in Equation 1.

Equation 1

$$m\ddot{x} + c\dot{x} + kx = 0$$

The back plate can be represented by a flat plate of constant thickness that is fixed at the inner radius to the fan mounting hub. The bolted connection between the fan mounting hub and the back plate is modeled by equivalent stiffness. Equivalent stiffness from the bolted connection is represented by two springs in parallel. The two stiffness elements are comprised of the tensile load of the bolt and the clamping force. Figure 4 illustrates the equivalent stiffness of the back plate connections.

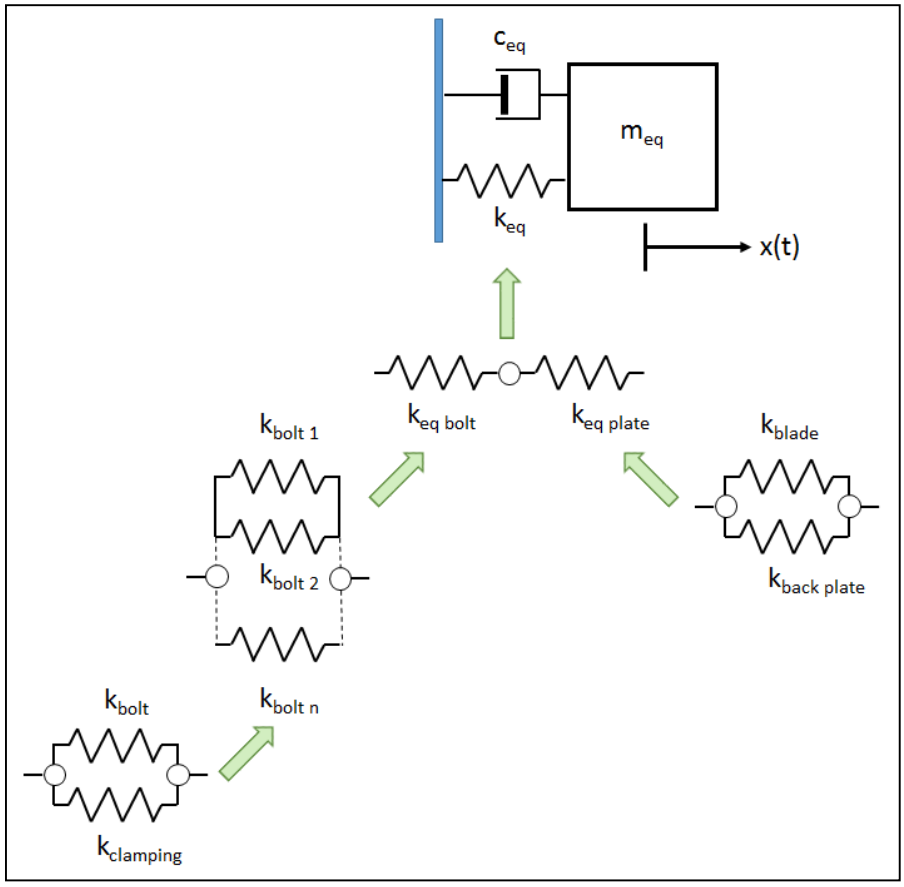

Figure 4. Schematic of single DOF representation of fan rotor with equivalent stiffness of connections.

In the SDOF closed form solution the stiffness of one bolted connection is varied to investigate the change in the fundamental natural frequency. The natural frequency is given by Equation 2.

Equation 2

$$\omega_n = \sqrt{\frac{k_{eq}}{m_{eq}}}$$

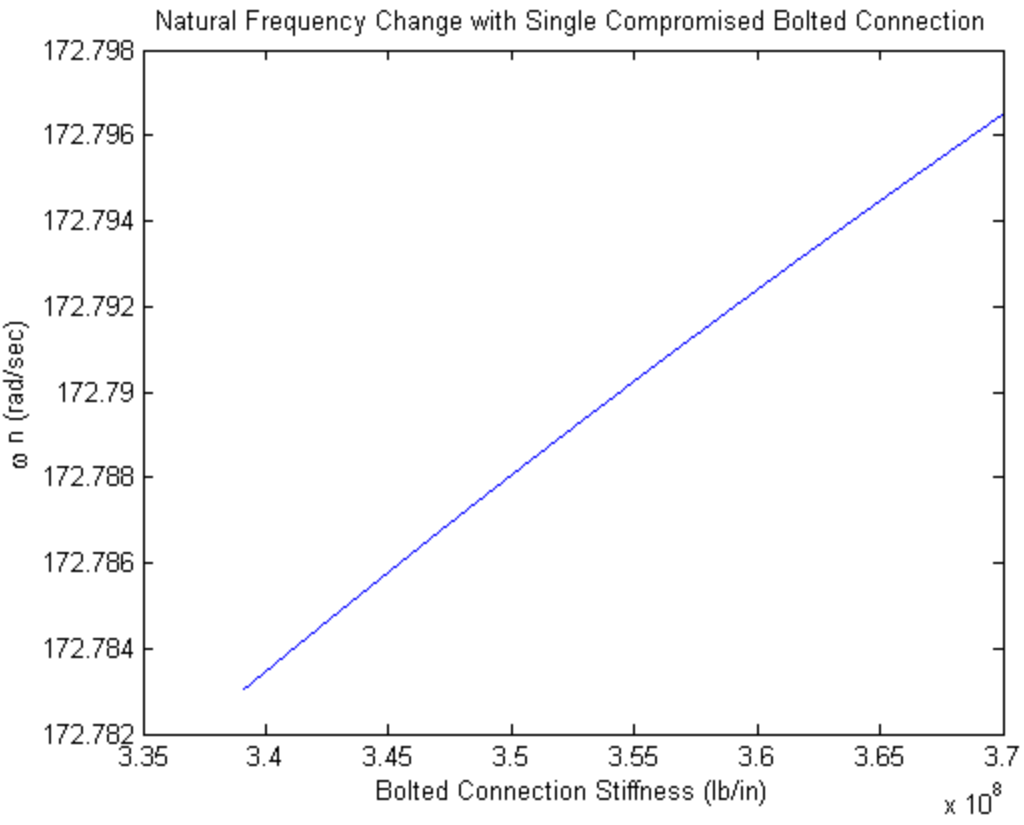

Figure 5. Plot of natural frequency for SDOF model with single compromised bolted connection.

Bolted connection stiffness, $[k_{eq}]$ in Equation 2, is varied by changing the contribution from one of twelve fasteners. The stiffness contribution of a single fastener is varied from zero stiffness up to the full theoretical stiffness of the bolted connection. This resulted in the range of bolted connection stiffness shown in Figure 5. A complete summary of all calculations is included in Appendix A. MATLAB was used to plot the results shown in Figure 5. The SDOF closed form solution shows insignificant changes to the natural frequency of the plate. The result is not surprising given the over simplification to a SDOF model. In a multi degree of freedom (MDOF) system tested by Wolff and Richardson, it was shown that changes in stiffness from the removal of a fastener will substantially affect stiffness and mode shapes (Wolff & Richardson, 1989).

In order to accurately test the effects on a MDOF system, experimental data is collected on the fan rotor assembly. The data are then utilized to extract natural frequencies, damping, and mode shapes. The experimental data collected represent the complex interactions of components making up the actual fan rotor. Figure 6 shows these components including the mounting hub, bolted connections, back plate, blades, and shroud with rib stiffener.

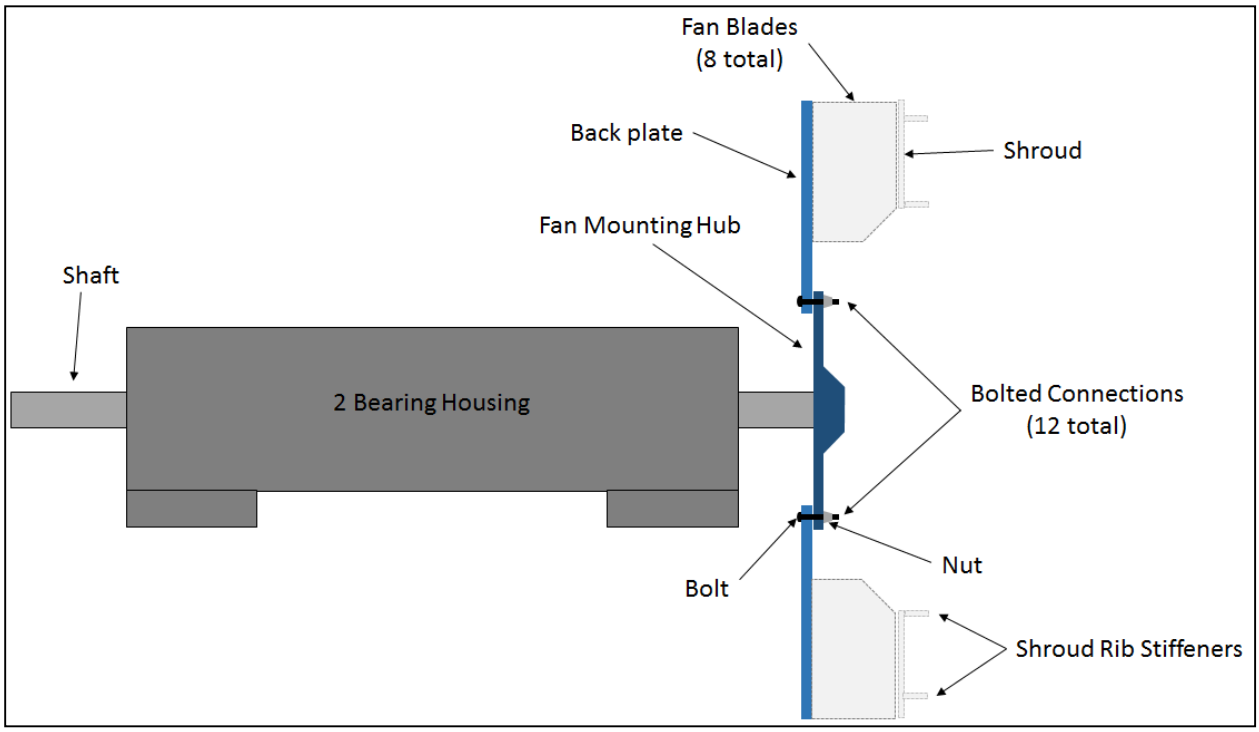

Figure 6. Schematic of fan assembly showing all components of the fan wheel.

Experimental Approach

Experimental data is utilized to determine if a loose fastener in an industrial fan rotor will change natural frequency or damping significantly enough at discrete locations to use as a structural health monitoring parameter. The goal of the experimental approach is to outline a test procedure that can be implemented in a manufacturing environment during a typical shutdown opportunity. The approach requires changes to natural frequency and damping to be evident in global modes so they can be detected at nearly any location on the structure. This minimizes the number of collection locations required.

All experimental data are collected on an industrial fan assembly from a glass manufacturing facility. The general experimental approach utilizes the fan rotor mounted to a rigid base. The mounted condition closely mimics in-situ conditions of the manufacturing environment. Accelerometers mounted to the back plate of the fan measure vibration response data from a modal hammer impact. Data are processed to calculate frequency response functions (FRF's). Subsequent curve fitting of the FRF data extracts modal frequencies, damping, and residues. This procedure is repeated for multiple iterations to determine the difference between an as-built configuration and a single bolt removed from the back plate. The data are then input into a program which is utilized to animate mode shapes. The animation of the mode shapes aids in determining global modes versus local modes. A global mode is one that affects nearly all locations on the test structure, and by viewing animations of the mode shapes they are easily recognized.

A few dominant global modes are used to compare global data from multiple test iterations. These results show whether a removed fastener affects the global natural frequencies, damping, and mode shapes. Individual collection locations are then compared to determine if similar changes are apparent in local data. The comparison of discrete collection locations is necessary to determine if a test procedure can be developed for use at a manufacturing plant.

Data are also collected on the rotor at a sample of discrete locations while varying the torque of a bolt. The varying torque of the bolt represents different degrees of clamping force provided by the bolted connection and therefore varying levels of a compromised connection. This data are compared to determine the sensitivity of the modal parameters to varying degrees of damage.

Repeatability of results is determined by repeating the entire process. The first bolt to be removed from the motor is replaced and re-torqued. Data are then collected on the entire rotor assembly with the replaced bolt and a second iteration is performed with a different removed fastener. Data are processed and analyzed the same as the previous test.

Experimental Procedures

The experimental procedures play an important role in determining if the experimental approach will be feasible in a manufacturing plant. For the purpose of this study a lab test setup was utilized to acquire and process data. The lab test setup is used to allow significant amounts of data to be collected for validation of the test procedure. The experimental procedure is broken down into multiple sections including test setup, instrumentation, detailed testing process, and data processing. Prior to the lab experimental procedure, unique considerations for application in a manufacturing plant are reviewed. The manufacturing plant testing will be referred to as in-situ testing from this point forward.

In-situ Testing Setup

The in-situ test setup requires that considerations be made to ensure testing time is kept to a minimum. A typical short duration shutdown opportunity at a glass manufacturing facility will range from fifteen minutes to one hour for access to the mold cooling fans. During shutdowns time is needed for the mold cooling fan to be de-energized for safe access to the fan rotor, leaving anywhere between 5 minutes and 50 minutes to complete testing. Given this time constraint a test procedure is desired that could be completed in approximately 5 minutes.

Access to the rotor is limited by a small removable panel on the side of the fan housing directly radial from the rotor. The opening measures approximately 6 inches wide by 12 inches tall. This access panel is provided on most industrial fans for quick access. There are no other access

panels that can be removed in a reasonable amount of time to gain more significant access to the fan rotor. The clearance between the fan rotor and the fan housing also limits data collection locations to the inside of the fan back plate.

Figure 7. In-situ collection location on the fan back plate.

Figure 7 shows a representation of the access to the fan rotor for testing. The shaded area around the perimeter represents the fan housing and the unshaded area represents the access panel opening. Magnet mounting of the accelerometers to the inside of the back plate allow for quick setup time and can be done with the access provided. Excitation of the rotor is performed by a modal hammer due to the simplicity of setup and the ability to use through the housing access panel. The location of the impact is determined based on a location that can be accessed through the fan housing panel. The alternative excitation method of a shaker and stinger would require more setup time and access to the rotor would make it very difficult to implement.

In addition to the instrumentation used the number of collection locations must be considered. To complete the testing in the time allowed all sensors must be placed and data collected simultaneously with one set of data. This limits the test setup to one excitation channel and potentially up to eight response measurements. Ideally one impact location and one response location would be collected as it represents the quickest setup and collection. This would also allow for the use of a commercially available 2 channel portable analyzer, which is also used for routine vibration condition monitoring. A portable analyzer is a preferred instrument for manufacturing environments because it is a robust, compact, battery powered instrument. If more than one response location is necessary more acquisition channels would be required on the recording device to obtain simultaneous data and a larger multi-channel recorder would need to be used. Higher channel count recorders typically require a plug in power source or a connection to a laptop making them less portable. Figure 8 shows a portable data collector on the left and a multi-channel recorder on the right.

Figure 8. Portable 2-channel data collector and multi-channel recorder.

Lab Testing Setup

A fan rotor utilized in a manufacturing plant setting was identified that could benefit from SHM to identify compromised bolted connections of rotor components. A complete fan assembly that

was no longer in service was obtained from a manufacturing plant for the purpose of this testing. The complete assembly consists of the fan rotor mounted to a shaft that is supported by two bearings contained within a common housing. In-situ the bearing housing is mounted to a rigid structural base and coupled to an AC Induction drive motor. The lab test setup uses a substantially rigid base to mount the fan assembly to adequately represent the in-situ conditions. In the lab test setup the fan is not coupled to a drive motor. Global modes of the fan back plate are the focus of the experimental approach. The absence of a coupled motor does not affect the mounted condition of the fan back plate and will not affect the global modes.

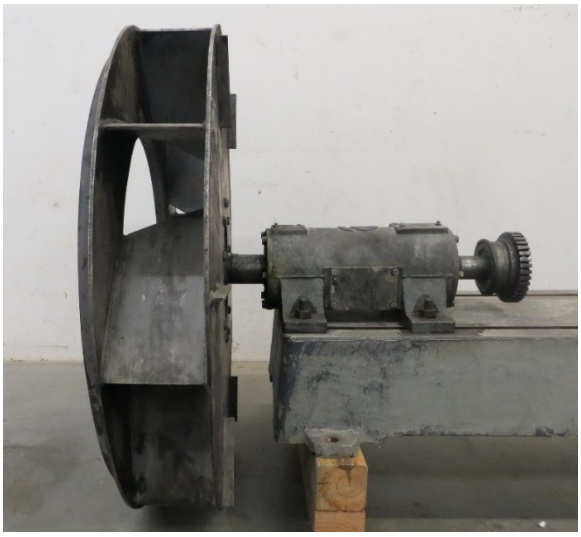

Figure 9. Fan rotor assembly used for lab testing.

The lab test setup is illustrated in Figure 9. The bolted fasteners, which will be the focus of the compromised component in this study, connect the back plate to the fan mounting hub. The mounting hub then attaches to the fan shaft. Twelve fasteners attach the back plate to the mounting hub. Each fastener is a 3/8 inch Magna-Grip button head MGPB "lock bolt" from Alcoa fastening systems. The head and collar of the bolt have a ¾ inch diameter clamping surface.

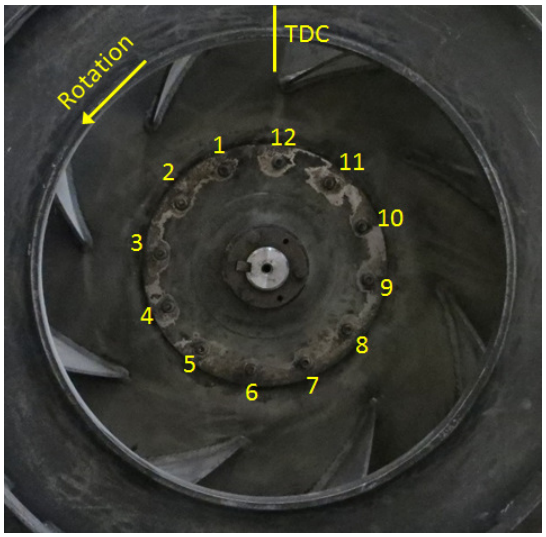

Figure 10. Bolts connecting the back plat to the mounting hub.

Figure 10 shows the identification of each fastener by numbering them from top dead center starting at one and proceeding counterclockwise through fastener twelve. The first iteration of removing a fastener removes bolt 10 and the second iteration removes bolt 2. These fasteners are ribbed fasteners with a permanent locking collar providing the clamping force similar to a threaded nut. To investigate the effect of varying torque on the rotor the removed fastener is replaced with a 3/8 inch threaded bolt. The bolt has a flange head and flange nut of equivalent ¾ inch diameter clamping surface.

Structural health monitoring requires the determination of modal parameters which are extracted experimentally using frequency response functions (FRF's). An FRF is a frequency domain function that describes the dynamic properties between a response and an excitation. A single input multiple output (SIMO) modal data set is collected to represent the structure. This requires a single point excitation source and multiple response locations. The excitation source is an impact hammer that requires no mounting to the structure and can be readily applied to this

application. The hammer can also be maneuvered through the access panel in the fan housing and excite many locations on the back plate. Determination of excitation location, called the driving point, is critical to provide adequate response throughout the structure. Therefore, many different locations must be accessible for determination of the driving point.

Response data are collected using accelerometers mounted to the fan back plate and hub using magnetic bases as shown in Figure 11. This allows for quick and repeatable placement of the accelerometers. During the lab test setup these sensors are placed on the outside of the fan back plate for unrestricted access to a full collection grid. Accelerometers are placed on the inside of the fan back plate for in-situ testing due to access and space constraints.

Figure 11. Placement of accelerometers on the fan back plate.

A response collection grid is defined on the fan back plate, shown in Figure 11 and illustrated in Figure 12, to be able to clearly define mode shapes of the structure. The collection grid is defined by 24 angular lines with 6 radial lines on the back plate and 2 radial lines on the mounting hub. The back plate and mounting hub, shown in Figure 12, are colored green and red,

respectively. The points at the intersection of grid lines represent each data collection location totaling 192. The point at the top dead center outer rim of the back plate represents the best driving point.

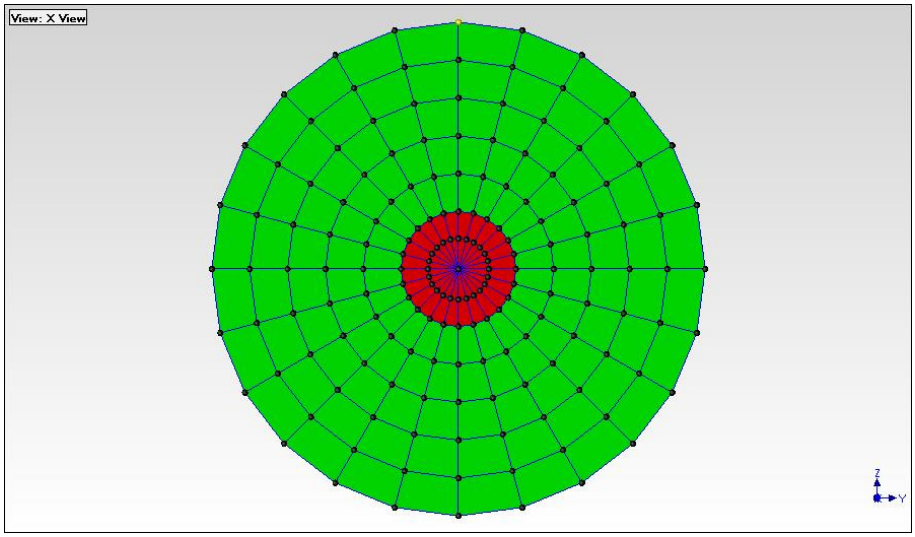

Figure 12. Response collection grid on the mounting hub (red) and the back plate (green).

All 192 locations signify the full collection grid of response measurements. In order to collect all grid locations 8 sensors are placed along an angular line and data is then collected. Sensors are then roved to the next 8 collection locations. This is repeated 24 times to collect all 192 locations. All data are then appended to one data file to represent FRF measurements from a complete response grid.

The effect of fastener torque is also considered in this study. The test setup is similar to the full collection grid, however only 8 collection locations are utilized for local data comparisons. The 8 locations are spread across the back plate to represent a potential in-situ setup. These collection locations are shown in Figure 13 with their point numbers indicated.

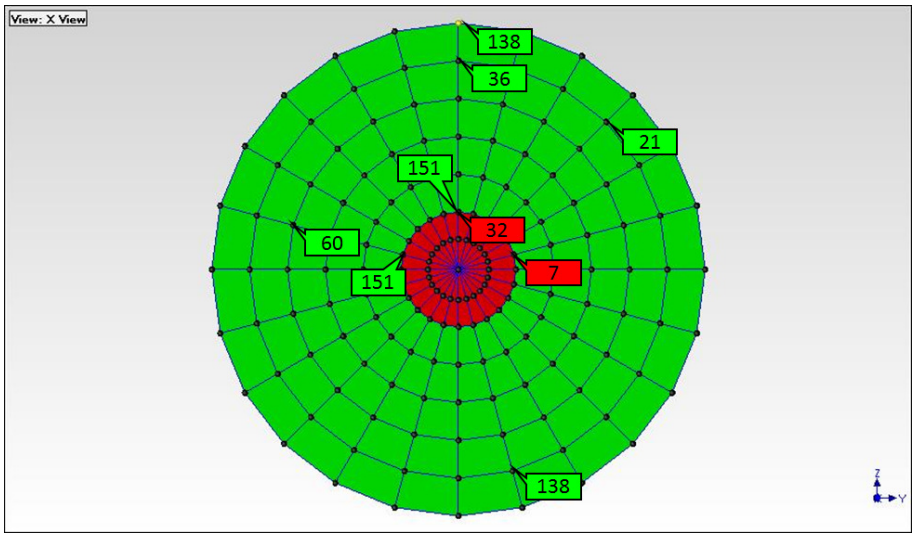

Figure 13. Discrete collection locations used for local data comparisons.

Instrumentation

Instrumentation was chosen to reflect typical hardware and software used in industrial manufacturing plants. Response data is captured using 100 mV/g single axis IMI precision ICP® accelerometers with a frequency response range from 0.58 to 6000 Hz. Their amplitude deviation is less than ±5% in this range. Sensors are full trace calibrated and have a measurement range of ± 50 g's with a broadband resolution of 50 µg. Curved surface magnets with a pull strength of 15 lbf are used to mount the transducers. A total of 8 accelerometers are used to capture response data simultaneously.

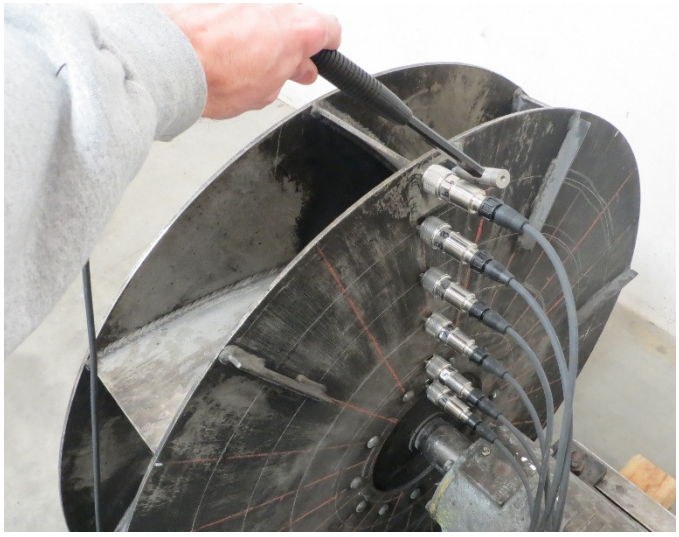

Figure 14. Accelerometers mounted with magnets and modal impact hammer.

An IMI 10 mV/lbf Modally Tuned® ICP® impact hammer is used to excite the rotor. The hammer has a measurement range of ± 500 lbf peak. Figure 14 shows the accelerometers mounted with magnets and impact hammer.

All data is conditioned by an NI PXI-4472B module capable of IEPE signal conditioning. The modules are controlled by a NI PXI 1033 chassis with integral controller. A PCMCIA Express data transfer card interfaces the NI PXI acquisition system with a laptop for communication with Vibrant's ME'scopeVES. The PXI acquisition system simultaneously acquires 9 channels up to 102.4 kS/s with a 24 bit A/D converter. Figure 15 shows the test setup. The fan rotor with magnet mounted accelerometers is on the left, PXI acquisition system in the center, and laptop with ME'scopeVES on the right.

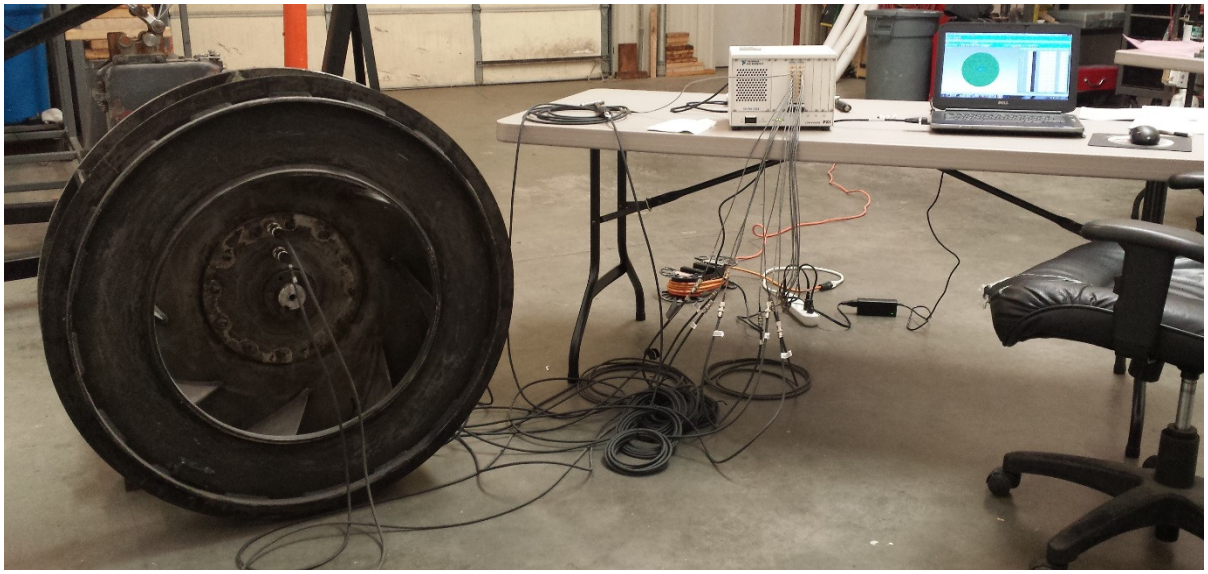

Figure 15. Instrumentation setup for data collection.

Data is streamed from the PXI acquisition system directly into ME'scopeVES software for data processing and digital storage of data. ME'scopeVES software is used to process time and frequency domain data as well as calculate FRF, auto spectrum, and coherence data of each degree of freedom (DOF).

Detailed Experimental Procedure

1) Mount fan assembly
    a) Bolt fan bearing housing to slotted test bed.
    b) Ensure fan rotates freely and no interferences are present that could change stiffness or add damping.
2) Instrumentation Setup

a) Connect PXI acquisition system to laptop with PCMCIA Express card. Power on PXI unit then power on laptop.

b) Connect ICP® impact hammer to channel 1with BNC extension cable.

c) Connect 8 ICP® accelerometers to channels 2 thru 9. Label all sensors and record transducer sensitivity.

d) Check functionality of data transfer, modal hammer, and all accelerometers.

3) ME'scopeVES Software Setup

a) Create wireframe structure of fan back plate and mounting hub. Mesh structure to include 24 angular lines on both the back plate and mounting hub. Mesh hub with 2 radial lines and back plate with 6 radial lines. Points are created at each mesh node as part of the meshing.

b) Create acquisition setup

i) Connect ME'scopeVES to PXI front end 4472B cards

ii) Setup input channel signal processing parameters.

(1) Apply 4 mA transducer power for all 9 channels to provide ICP (IEPE) sensor power.

(2) Use AC coupling of all channels to remove the DC bias voltage from the sensor power.

(3) Set units to [lbf] for channel 1 and [g] for channel 2 thru 9.

(4) Set proper transducer sensitivity for each channel. Channel 1 XXX [mV/lbf], channel 2 thru 9 XXX [mV/g], where XXX refers to transducer sensitivity included in appendix B.

(5) Set channel 1 as “input” and channels 2 thru 9 as “output”. Input is designated for the reference measurement which all DOF’s will be measured against for FRF calculations. In this experimental approach the hammer excitation is the input and the accelerometer responses are the output.

(6) Apply a force window to channel 1 to minimize noise from the impulse signal. The impulse should only be a single short duration event with zero amplitude prior to and following the impulse. The force window preserves the impulse and assumes any non-zero data after the impulse is noise and forces the amplitude to zero.

(7) Apply a rectangular window to channels 2 thru 9 if the ring down is completely contained within the time sample of data. Apply an exponential window if the data does not decay to zero within the time sample of data. An exponential window forces the amplitude of the signal to decay to zero within the time sample. This minimizes leakage in the frequency domain caused by a non-periodic function. The exponential window applies an artificial damping to the data which must be compensated for during data post processing to obtain accurate damping results. If the data decays to zero within the time sample a rectangular window is preferred so artificial damping is not introduced. All data collected in this experimental approach decayed within the time sample and therefore a rectangular window is applied.

(8) Setup frequency domain measurements and select Auto spectrum, FRF, and coherence to be calculated from measured data. Even though frequency domain measurement are made, time waveform samples are also saved during collection.

Three linear averages should be specified to provide more accurate results and remove measurement noise for variation of impacts.

(9) Specify a frequency span maximum frequency of 2050 Hz and 32768 samples for each data block. ME'scopeVES software performs a Fourier Transform, as opposed to a Fast Fourier Transform, on all time domain data to convert to the frequency domain. To prevent aliasing of the signal the software utilizes an anti-alias filter and doubles the time domain sampling. Given the software does not add additional samples to account for roll off of the filter a frequency span is specified that will not utilize the upper end of the frequency range (Ewins, 2000). A high number of samples is selected to produce a long time sample period to ensure the data decay's to zero within the time sample and also provide good spectral resolution.

(10) Set channel 1 as the trigger source and estimate a trigger level. Acquire data to test the trigger level by impacting the object with the anticipated tip to be used in testing. Adjust the trigger level to equal approximately half of the impulse force exerted on the structure.

(11) Set a pre-trigger to acquire samples leading up to the trigger event. This is necessary to ensure the impulse and response signals are periodic signals to prevent leakage. A periodic signal is one that experiences a complete number of cycles, which in this case will hold true if they start and end with zero amplitude.

iii) Determine proper impact hammer tip

(1) Starting with the softest hammer tip collect FRF's, coherence data, and auto spectra with accelerometers placed at a wide array of locations on the fan back plate.

(2) Review the data for quality over the frequency range of interest.

(3) Repeat the process with increasing hardness of tips. Choose the softest tip that excites the frequency range of interest and produces the best quality data.

iv) Determine excitation driving point

(1) Identify an excitation location on the structure that will not be a node in as many global mode shapes as possible.

(2) Impact the structure at this location and collect FRF's, coherence data, and auto spectra with accelerometers placed at a wide array of locations on the fan back plate.

(3) Review the data for quality over the frequency range of interest.

(4) Repeat the process testing other excitation locations. Choose an excitation location that provides the best quality of data at the most response locations as possible.

v) Collect initial set of data and check the data quality using the following checks.

(1) Check the impulse time waveform and ensure no double hits are present. Also ensure no noise is present surrounding the impulse.

(2) Check the response time waveform and ensure the response rings down within the time sample. Check pre-trigger duration to ensure multiple samples of zero amplitude are present at the beginning of the time sample. Also check for double

hits indicated by multiple ring down events. Ensure background noise is not present.

(3) Check the coherence plot of each DOF and ensure the frequency range of interest maintains coherence above 0.9 except for sharp dropout at resonant and antiresonant frequencies that immediately return to amplitudes above 0.9.

(4) Check the FRF data of each DOF and ensure smooth traces with clean distinct resonant and antiresonant peaks. Overlay all traces and look for repeatability between DOF's.

vi) Collect data at all collection locations

(1) Place 8 response sensors at 8 grid locations. Record location and sensor orientation for each channel. Ensure transducer direction, positive or negative, is recorded accurately. This defines the degree of freedom of each measurement.

(2) Impact the rotor at the driving point. Repeat 3 times to collect 3 averages of impact data.

(3) Verify quality of data by a quick check of the FRF's and coherence plots.

(4) Save data to a new data block.

(5) Move sensors to new grid locations. Record location and sensor orientation for each channel.

(6) Repeat steps (2) and (3).

(7) Save data to previous data block created.

(8) Repeat steps (5) thru (7) until all location are collected.

vii) Overlay all FRF traces from data block and identify outliers. Recollect poor data as necessary.

viii) Create animation equations and animate structure at dominant global modes. Check data quality by looking for discrete points that animate significantly different than adjacent points. Recollect points if necessary.

4) The full grid collection procedure is repeated for 4 different rotor configurations.
   a) The as-built rotor with no alterations to it. (As Built)
   b) The rotor with bolt number 10 removed from the fan back plate. (Bolt 10 Removed)
   c) The rotor with bolt number 10 and bolt number 2 replaced by threaded fasteners and torqued to 40 ft-lb. (Bolt 10 and 2, 40 ft-lb)
   d) The rotor with bolt number 10 replaced by a threaded fastener and torqued to 40 ft-lb and bolt 2 removed. (Bolt 2 Removed)
   e) An abridged collection consisting of points, 7, 21, 32, 36, 60, 101, 151, and 161 is used to collect local FRF data while varying bolt toque. The collection procedure is the same as step 3) with the exception of the limited testing points. The procedure is performed on the rotor with bolt number 10 replaced by a threaded fastener and collections made with bolt torque set to 0 ft-lb, 10 ft-lb, 20 ft-lb, 30 ft-lb, 40 ft-lb, and 50 ft-lb.

Data Processing

Data processing is completed using ME'scopeVES software by Vibrant Technologies. During data collection; FRF, coherence, and auto spectra are automatically calculated from frequency domain data by the software.

Additional processing of the data includes curve fitting of the experimental data to extract modal frequencies, damping, and residues. The residues that define the shapes are saved to a shape table for comparison using Modal Assurance Criterion, referred to as MAC. MAC is a scalar quantity that provides a measure of the least squares deviation of data from exact correlation. It is computed from two data sets to determine correlation between them. A value of 1.0 is expected for two identical mode shapes. In application, a value of 0.9 (90%) would be considered good correlation (Ewins, 2000) (Vibrant Technology, Inc., 2001).

Analysis Procedures

The following are the specific analysis procedures implemented to post process data in ME'scopeVES. Data are first globally curve fit and then discrete DOF's are locally curve fit. Global curve fitting uses FRF data from all DOF's to identify an average natural frequency and damping for the entire set of data. It then uses this natural frequency and damping for calculation of residues for each DOF. Local curve fitting uses one FRF trace that represents one DOF and identifies the natural frequency and damping of the individual trace.

1) Global Curve Fitting is performed to provide insight as to whether the global mode shapes, natural frequencies and damping are affected by a removed fastener.
    a) All FRF's are overlaid to be used for curve fitting.
    b) Cursors are placed to specify a discrete frequency range to curve fit. This allows global modes to be focused on in the curve fitting process. A complex structure may have many natural frequencies, all of which will not be global modes. The fan rotor in this study has

numerous natural frequencies so the most dominant global modes are focused on for global curve fitting.

c) Using the complex mode indicator function (CMIF) the software counts the peaks within the frequency range of interest. Amplitude threshold limits are adjusted to avoid peaks produced by noise within the FRF data. CMIF is the singular value decomposition of the FRF sub matrix. The mode indicator values are provided by the squares of the singular values plotted against frequency. The natural frequencies are indicated by the highest values of the first CMIF. (Ewins, 2000) (Vibrant Technology, Inc., 2001)

d) Using a global polynomial method the frequency and damping of each peak are calculated.

e) The polynomial method is then used to calculate residues of each DOF for the frequency determined in the previous step. The residue represents a vector containing a magnitude and phase angle for each DOF. The combination of the residues for every DOF was then saved as a mode shape.

f) Steps b) thru e) are then repeated for all frequency ranges of interest.

g) After all frequencies, damping, and mode shapes have been identified the results are saved to a shape table.

h) This global curve fitting process is repeated for the four iterations of data collected on the full grid.

i) The shape tables obtained from the curve fit data of the four iterations are then used to compute MAC values between the iterations.

2) ME'scopeVES software is used to animate and compare shapes from the global fit data.

3) Local Curve Fitting is performed to provide insight as to whether discrete data points can be used as a basis for SHM to identify a compromised connection.
    a) Individual DOF FRF's are used one at a time for curve fitting.
    b) Cursors are placed to specify a discrete frequency range to curve fit. This allows three dominant global modes to be focused on in the curve fitting.
    c) Using the complex mode indicator function (CMIF) the software counts the peaks within the frequency range of interest. Amplitude threshold limits are adjusted to avoid peaks produced by noise within the FRF data.
    d) Using a local polynomial method the frequency and damping of each peak are calculated.
    e) The polynomial method is then used to calculate residue for the DOF being utilized.
    f) Steps b) thru e) are then repeated for all frequency ranges of interest.
    g) After all frequencies, damping, and residues have been identified the results are saved to a shape table.
    h) This local curve fitting process is repeated for the 8 DOF's identified earlier and for the multiple iterations of fastener torque on bolt 10.

Results

The results of the experimental approach are summarized in two parts, global data comparisons and local frequency and damping results. Additional supporting data is contained in Appendix C.

Global Data Comparisons

Modal parameters obtained from the global curve fit of all DOF's are reviewed first to determine if there are significant changes in global frequencies, damping and mode shapes. The following comparisons are performed.

Case #1: As Built Compared to Bolt 10 Removed

This comparison is between the as-built rotor with no alterations to it and the rotor with bolt number 10 removed from the fan back plate.

	As Built	Bolt 10 Removed	
Mode	Frequency (Hz)	Frequency (Hz)	% Change
1	26.49	26.37	-0.5%
2	31.80	31.59	-0.7%
3	39.99	39.95	-0.1%
4	124.20	123.82	-0.3%
5	267.30	267.91	0.2%
6	594.26	592.86	-0.2%

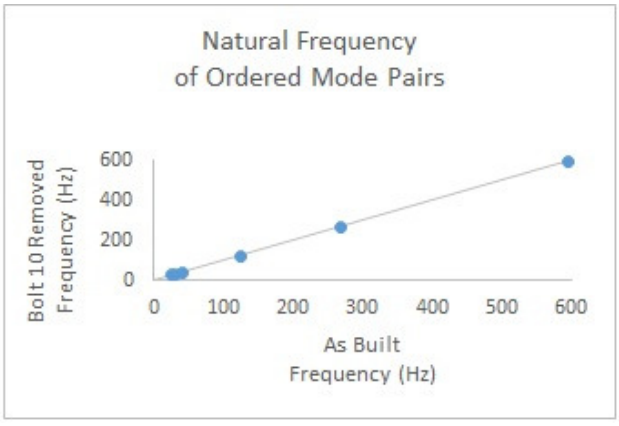

Figure 16. Natural frequency comparison between as built and bolt 10 removed.

The removal of bolt 10 from the rotor had negligible effects on the global natural frequencies as seen in Figure 16. Points that lie on the line of slope 1 indicate the same value between ordered mode pairs. Points scattered about the line indicate differences between values. Mode 6 was influenced the most with only a 0.7% change.

Mode	As Built Damping (%)	Bolt 10 Removed Damping (%)	% Change
1	2.02	0.95	-52.9%
2	0.74	0.70	-5.4%
3	1.65	2.61	58.2%
4	1.50	1.16	-22.7%
5	0.95	0.95	0.7%
6	0.16	0.21	29.9%

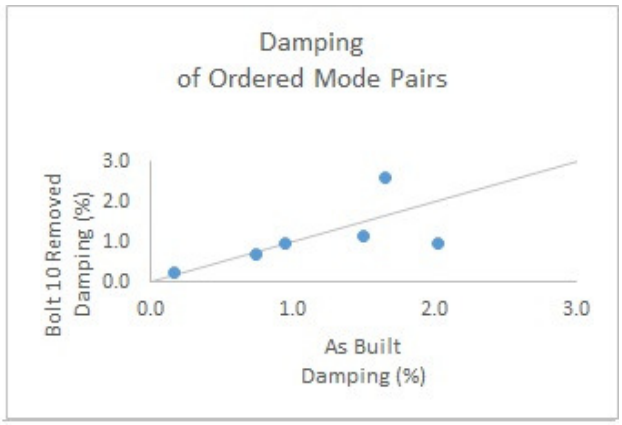

Figure 17. Damping comparison between as built and bolt 10 removed.

Damping did change significantly, up to 58%, with the removal of bolt 10 as illustrated in the plot of ordered pairs in Figure 17.

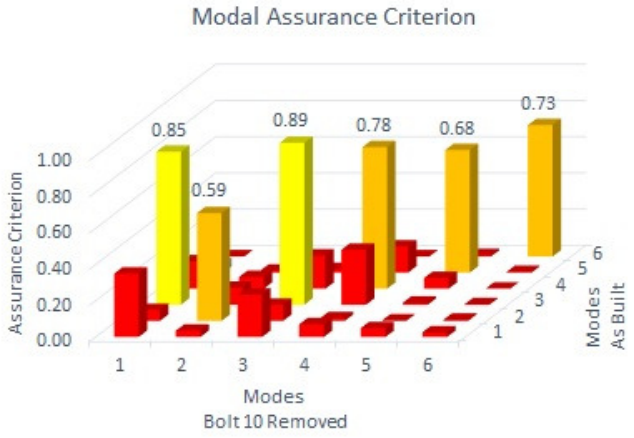

Figure 18. MAC between as built compared to bolt 10 removed.

Modal assurance criterion for case 1, illustrated by the MAC plot in Figure 18, showed significant sensitivity to mode shapes from the removal of bolt 10. MAC values of 1.0 indicate an identical mode shape since it signifies exact correlation between 2 experimentally measured mode shapes, $\{\varphi_X\}$ and $\{\varphi_Y\}$, given by Equation 3.

Equation 3

$$MAC(Y,X) = \frac{|\{\varphi_X\}^T\{\varphi_Y\}|^2}{(\{\varphi_X\}^T\{\varphi_X\})(\{\varphi_Y\}^T\{\varphi_Y\})}$$

The notation $\{\varphi\}$ represents a vector of values corresponding to the amplitudes of discrete points that as a vector make up the mode shape of an experimentally measured mode. This is the eigenvector (mode shape) that corresponds to a unique eigenvalue (natural frequency). Comparison of two sets of experimentally measured data, X and Y, produces a MAC value representing a comparison between each mode from set X with each mode from set Y. In application MAC values greater than 0.9 are considered similar mode shapes. Values under 0.9 represent mode shapes that are significantly different (Ewins, 2000) (Vibrant Technology, Inc., 2001). Only mode 3 approaches the 0.9 criteria for a similar mode shape. The other 5 modes are significantly different between the as-built rotor and the rotor with bolt 10 removed.

Case #2: Bolt 10 and 2, 40 ft-lb Compared to Bolt 2 Removed

Case #2 compares the rotor with bolt number 10 and bolt number 2 replaced by threaded fasteners and torqued to 40 ft-lb. This is compared to the rotor with bolt number 10 replaced by a threaded fastener and torqued to 40 ft-lb and bolt 2 removed. This comparison is performed to

determine if bolts removed from different locations on the rotor have a similar effect on modal parameters.

Mode	Bolt 10 and 2, 40 ft-lb Frequency (Hz)	Bolt 2 Removed Frequency (Hz)	% Change
1	26.08	25.90	-0.7%
2	31.72	31.42	-0.9%
3	40.19	40.01	-0.4%
4	122.14	121.47	-0.6%
5	267.71	265.43	-0.9%
6	592.63	591.71	-0.2%

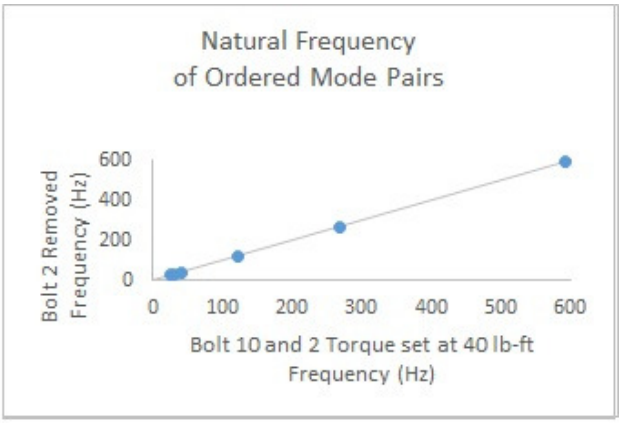

Figure 19. Natural frequency comparison between bolt 10 and 2, 40 ft-lb and bolt 2 removed.

The removal of bolt 2 from the rotor had negligible effects on nearly all global natural frequencies in case #2 as seen in Figure 19. Mode 5 was influenced the most with a change of 0.9 %. The change from the removal of bolt 2 influenced a different mode compared to case #1 and the removal of bolt 10. This result suggested the location of the removed bolt is also significant in the modal parameters of the fan rotor.

Mode	Bolt 10 and 2, 40 ft-lb Damping (%)	Bolt 2 Removed Damping (%)	% Change
1	2.08	1.60	-23.1%
2	0.65	0.74	14.3%
3	2.41	2.37	-1.7%
4	1.22	1.16	-4.9%
5	0.85	0.91	6.2%
6	0.15	0.15	0.7%

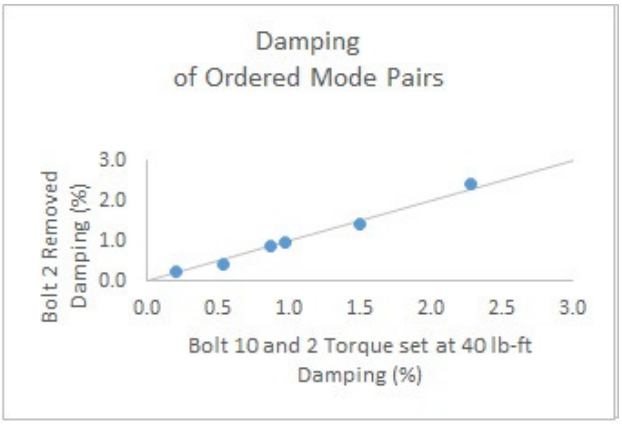

Figure 20. Damping comparison between bolt 10 and 2, 40 ft-lb and bolt 2 removed.

Damping changes for case #2 were minimal as shown in Figure 20. Similar to the frequency results, case #1 and case #2 produced different changes in the data from the removal of 2 different bolts.

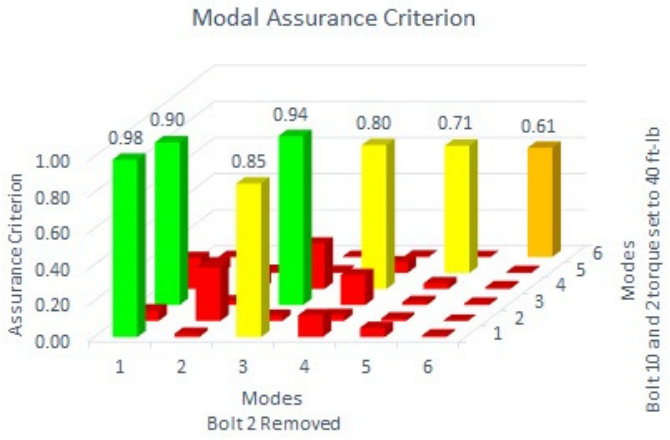

Figure 21. MAC between bolt 10 and 2, 40 ft-lb and bolt 2 removed.

Modal assurance criterion, shown in Figure 21, for case 2 produced multiple similar modes shapes between the two configurations in this case. Mode 1 and 3 were similar mode shapes as indicated by a MAC value of 0.98 and 0.94 respectively. The other 4 shapes showed significant sensitivity from the removal of bolt 2.

Case #3: As Built Compared to Bolt 10 and 2, 40 ft-lb

Case #3 compared the as-built rotor to the rotor with bolt number 10 and bolt number 2 replaced by threaded fasteners and torqued to 40 ft-lb. This comparison was performed to determine how closely the modified fasteners torqued to 40 ft-lb matched the as built configuration.

Mode	As Built Frequency (Hz)	Bolt 10 and 2, 40 ft-lb Frequency (Hz)	% Change
1	26.49	26.08	-1.6%
2	31.80	31.72	-0.3%
3	39.99	40.19	0.5%
4	124.20	122.14	-1.7%
5	267.30	267.71	0.2%
6	594.26	592.63	-0.3%

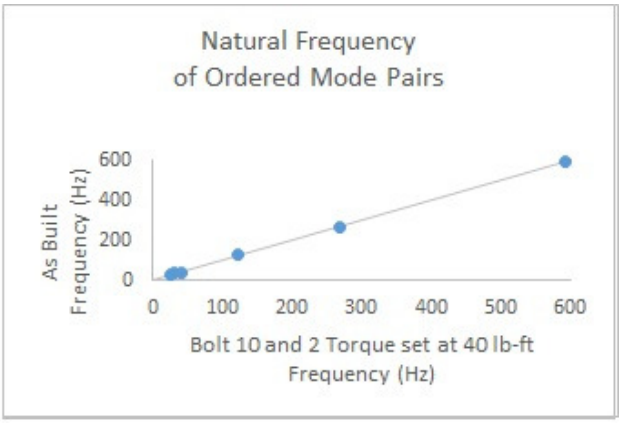

Figure 22. Natural frequency comparison between as built and bolt 10 and 2, 40 ft-lb.

The natural frequencies between the two configurations shown in Figure 22 experienced a maximum change of 1.7 %. This change is more than the frequency change experienced in case #1 and #2. The change in frequency indicates the modified fasteners do not match the as built configuration.

Mode	As Built Damping (%)	Bolt 10 and 2, 40 ft-lb Damping (%)	% Change
1	2.02	2.08	3.0%
2	0.74	0.65	-12.5%
3	1.65	2.41	46.1%
4	1.50	1.22	-18.7%
5	0.95	0.85	-9.8%
6	0.16	0.15	-10.4%

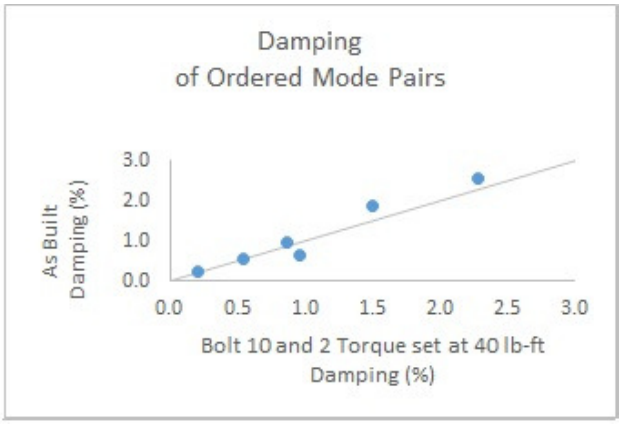

Figure 23. Damping comparison between as built and bolt 10 and 2, 40 ft-lb.

Damping differences between the as built and modified fasteners, shown in Figure 23, were within 20% in 5 of the 6 modes with a maximum change over 46%. The change between the two configurations was in between the changes of case #1 and #2. This change in damping also indicates the configurations are not similar.

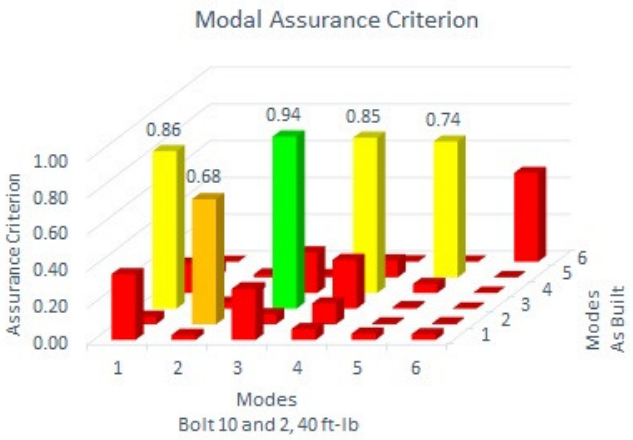

Figure 24. MAC between as built and bolt 10 and 2, 40 ft-lb.

The MAC comparison, shown in Figure 24, between the as-built rotor and the bolt 10 and 2 fasteners torqued to 40 ft-lb shows poor correlation for all modes except mode 3. This data indicates the modified fasteners torqued to 40 ft-lb are not an equivalent setup to the as-built rotor. Information obtained after all testing was complete indicated the factory Magna-Grip lock bolt clamp load averages 4000 lbs for the 3/8 inch fastener. Due to the permanent nature of the bolt this could not be determined during the removal of the Magna-Grip fastener. The threaded fastener used was a SAE Grade 8, 3/8 inch, 16 threads per inch bolt. Torqued at 40 ft-lb the threaded fastener has a calculated clamp load of 6222 lbs. The difference between the lock bolt clamp load and threaded fastener clamp load produces the modal parameter differences shown in case #3. This information also indicates why a single fastener removed in case #1 and case #2 did not produce similar results. In case #1 bolt 10 was removed and the remaining 11 fasteners were as-built lock bolt fasteners. In case #2 bolt 2 was removed with only 10 as-built lock bolt fasteners in place. One of the fasteners, bolt 10, was a threaded fastener torqued to 40 ft-lb in case #2. Given the threaded fastener torqued to 40 ft-lb does not match the bolted connection of

the as-built lock bolt, it shows more than one variable changed between case #1 and case #2. This produced varying results from the removal of a single fastener.

Case #4: Bolt 10 Removed Compared to Bolt 2 Removed

Data in case #4 is compared between the rotor with bolt number 10 removed from the fan back plate and the rotor with bolt number 10 replaced by a threaded fastener and torqued to 40 ft-lb with bolt 2 removed.

Mode	Bolt 10 Removed Frequency (Hz)	Bolt 2 Removed Frequency (Hz)	% Change
1	26.37	25.90	-1.8%
2	31.59	31.42	-0.5%
3	39.95	40.01	0.2%
4	123.82	121.47	-1.9%
5	267.91	265.43	-0.9%
6	592.86	591.71	-0.2%

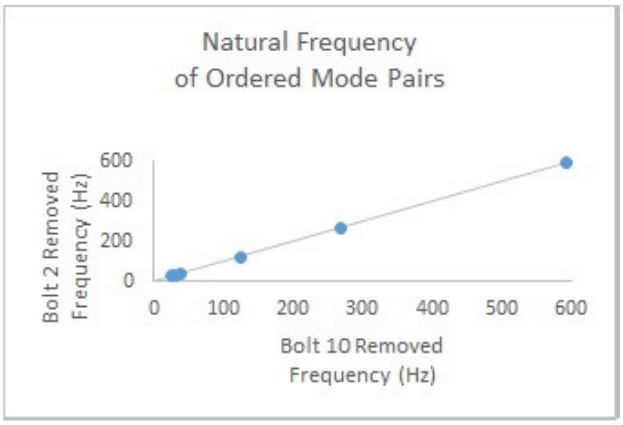

Figure 25. Natural frequency comparison between bolt 10 removed and bolt 2 removed.

The maximum frequency change between bolt 10 removed and bolt 2 removed was 1.9 % as shown in Figure 25.

Mode	Bolt 10 Removed Damping (%)	Bolt 2 Removed Damping (%)	% Change
1	0.95	1.60	68.1%
2	0.70	0.74	5.7%
3	2.61	2.37	-9.2%
4	1.16	1.16	0.0%
5	0.95	0.91	-4.9%
6	0.21	0.15	-30.5%

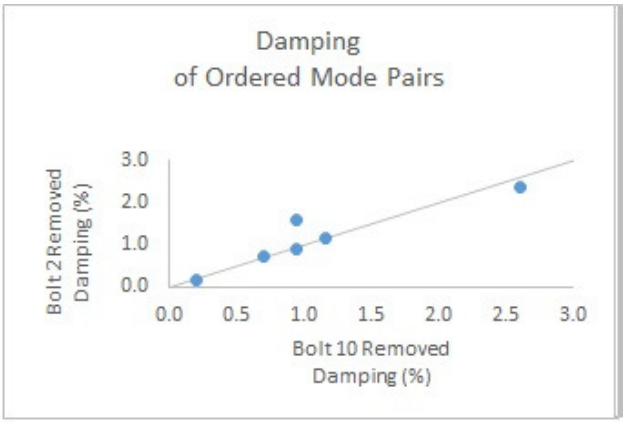

Figure 26. Damping comparison between bolt 10 removed and bolt 2 removed.

The damping changes between bolt 10 removed and bolt 2 removed were the most significant at mode 1 and 6, with changes of 68.1% and 30.5% respectively. Figure 26 illustrates these results.

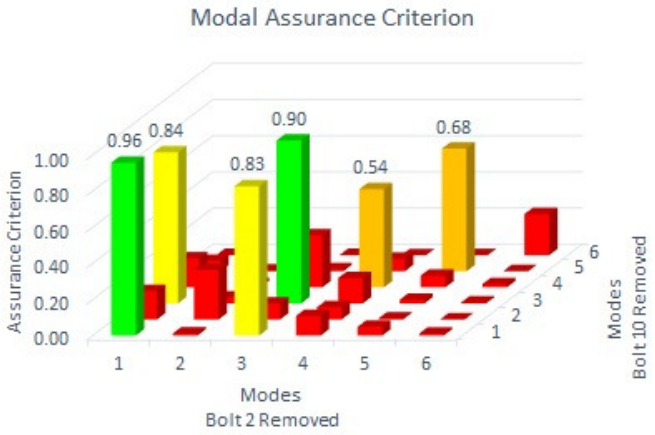

Figure 27. MAC between bolt 10 removed and bolt 2 removed.

MAC values for the two configurations shown in Figure 27 illustrate mode 1 and 3 had similar shapes. The other 4 modes were significantly different shapes. The differences in natural frequencies, damping, and modes shapes between the removal of bolt 10 and bolt 2 should not correlate. This is due to the removal of bolt 2 having the presence of bolt 10 as a threaded fastener torqued to 40 ft-lb. Case #3 illustrated how this was not an accurate approximation of the as-built rotor.

The results show that changes in fastener condition showed little to no influence on the natural frequency though damping and mode shapes were significantly influenced. The attempt to repeat the factory lock bolt configuration was not successful as indicated by the MAC values in case #3. Case #3 did continue to support the above conclusions from the results.

Local Frequency and Damping

Global data indicated the frequency will not change significantly due to a compromised fastener. The damping and modes shapes did however change significantly. The experimental approach requires that a procedure be developed which can be applied quickly. Given this constraint, mode shape comparisons are not utilized for in-situ testing due to the time consuming data collection required. As a result of this, local point data is the actual data obtained in the field for the application of SHM.

Local data from 8 collection locations was curve fit for 3 of the dominant modes, mode 1, 5, and 6. Point data is provided in Appendix C. The data presented in Figure 28 and Figure 29 show the significant variation from point to point for changes in frequency and damping. The average and standard deviation of the data illustrate these changes. The deviation in data was the same magnitude as the average percent change. Results of a typical local data set indicate SHM cannot be implemented in-situ on this rotor. The small data set of frequency and damping modal parameters is too inconsistent.

		Frequency % Change			
Mode		Case #1- As Built vs Bolt 10 Removed	Case #2 - Bolt 10 and 2, 40 ft-lb vs Bolt 2 Removed	Case #3 - As Built vs Bolt 10 and 2, 40 ft-lb	Case #4 - Bolt 10 Removed vs Bolt 2 Removed
1	Average	1.3%	0.1%	2.1%	1.0%
	Std Dev	0.8%	0.1%	1.3%	0.2%
5	Average	1.8%	0.2%	0.7%	1.4%
	Std Dev	1.0%	0.2%	0.7%	0.2%
6	Average	0.2%	0.2%	0.2%	0.1%
	Std Dev	0.2%	0.0%	0.2%	0.0%

Figure 28. Average and standard deviation of frequency differences for discrete DOF's.

		Damping % Change			
Mode		Case #1- As Built vs Bolt 10 Removed	Case #2 - Bolt 10 and 2, 40 ft-lb vs Bolt 2 Removed	Case #3 - As Built vs Bolt 10 and 2, 40 ft-lb	Case #4 - Bolt 10 Removed vs Bolt 2 Removed
1	Average	18.8%	26.8%	26.4%	18.0%
	Std Dev	15.1%	19.5%	12.5%	14.3%
5	Average	29.1%	16.0%	27.0%	66.7%
	Std Dev	11.2%	13.5%	23.4%	14.3%
6	Average	27.0%	5.9%	114.5%	124.7%
	Std Dev	24.4%	6.7%	54.4%	16.1%

Figure 29. Average and standard deviation of damping differences for discrete DOF's.

Local data of 8 data points was also used to investigate the effect of fastener torque on the frequency and damping modal properties. The fastener torque was not found to significantly affect the natural frequency but it did significantly affect the damping. The point to point variation of damping data is illustrated in Figure 30 and Figure 31. Some local points showed significant differences while others showed no differences. Additionally, the variation from point to point was not consistent so specific collection locations cannot be identified for the purpose of the SHM.

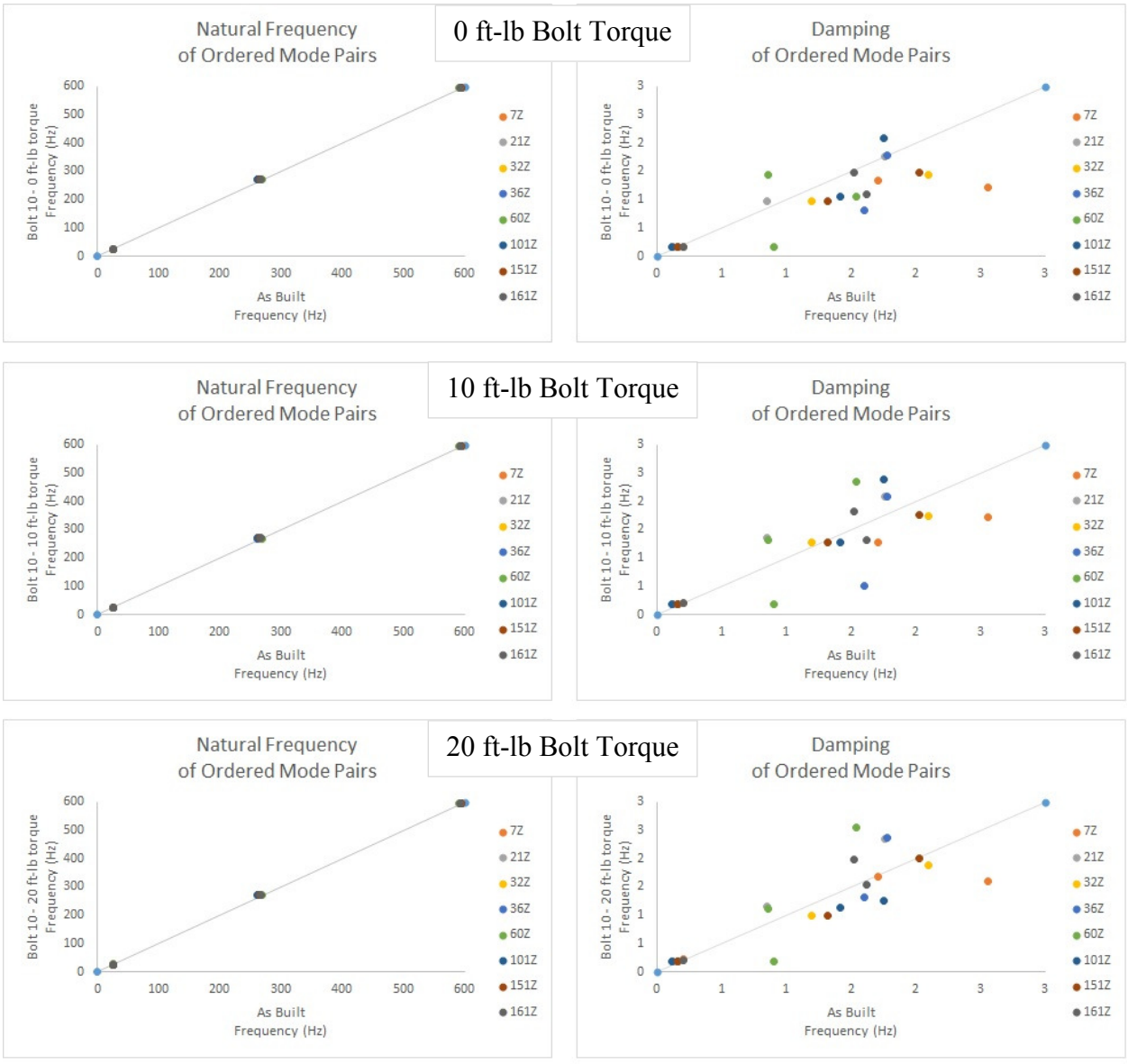

Figure 30. Bolt 10 varying fastener torque 0, 10 and 20 ft-lb.

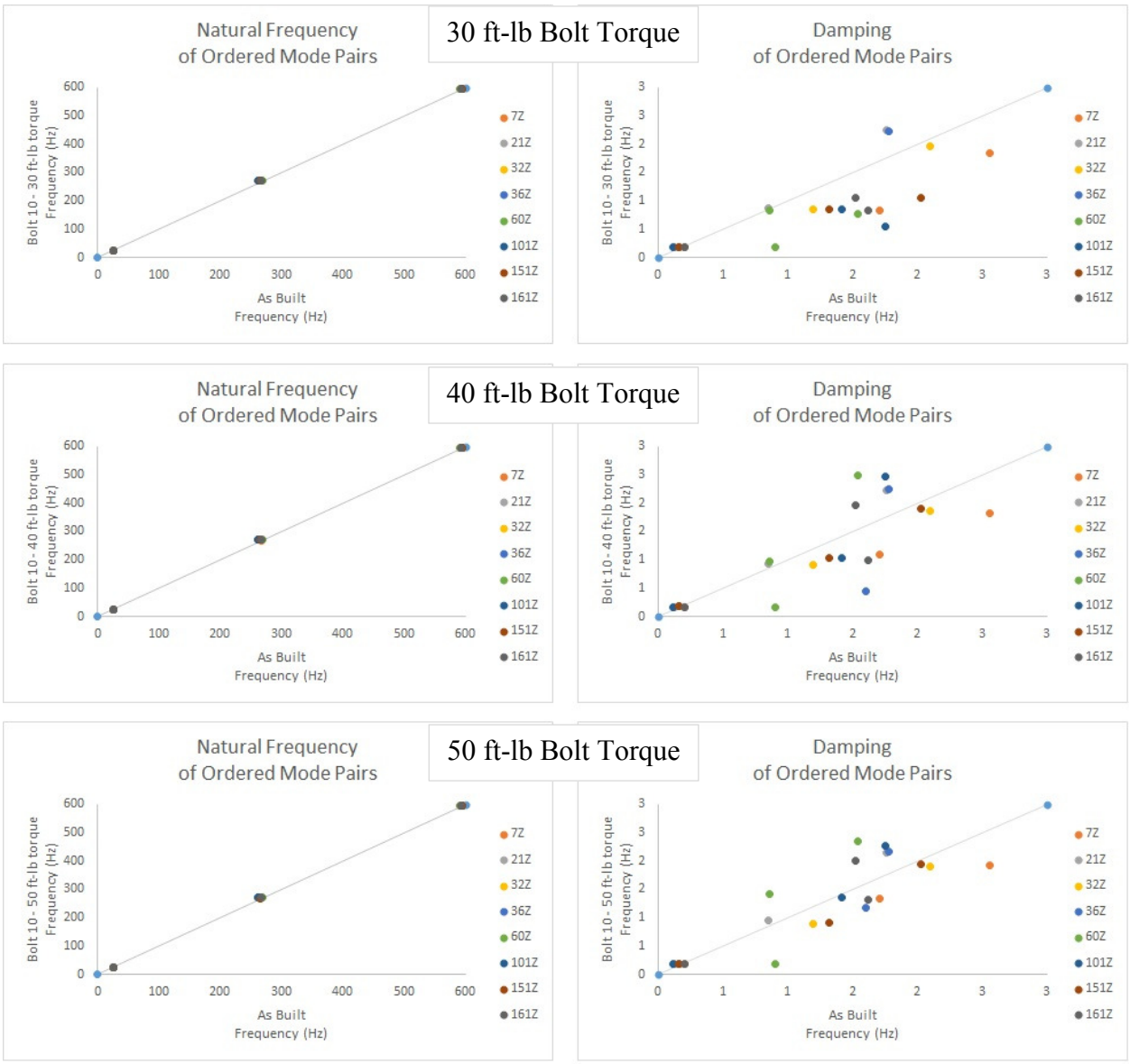

Figure 31. Bolt 10 varying fastener torque 30, 40 and 50 ft-lb.

Errors and limitation of results

Data collected in this study is subjected to review to ensure signal quality, signal fidelity, measurement repeatability, and measurement reliability (Ewins, 2000). These are areas used to verify the quality of the measured data and are applied to the experimentally measured data here.

Signal quality refers to obtaining adequate strength and clarity in the data. Time waveform, auto spectrum, FRF, and coherence data are reviewed to verify signal quality. The overlay of time waveforms, shown in Figure 32, from the impact data show a single impact with leading and trailing zero's and no noise around the impulse.

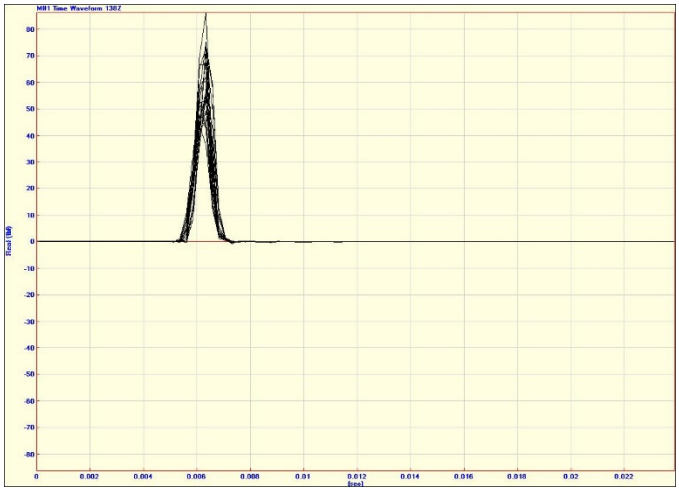

Figure 32. Overlay of impulse time waveforms.

The time waveform shown in Figure 33 illustrates the quality of the response data with a clean excitation and ring down contained within the time sample period. This removes the need for an exponential window that would apply artificial damping. The rectangular window, also referred to as a boxcar window, is used in this case to maintain accurate damping. Both the impulse and response waveforms are clear of double hits.

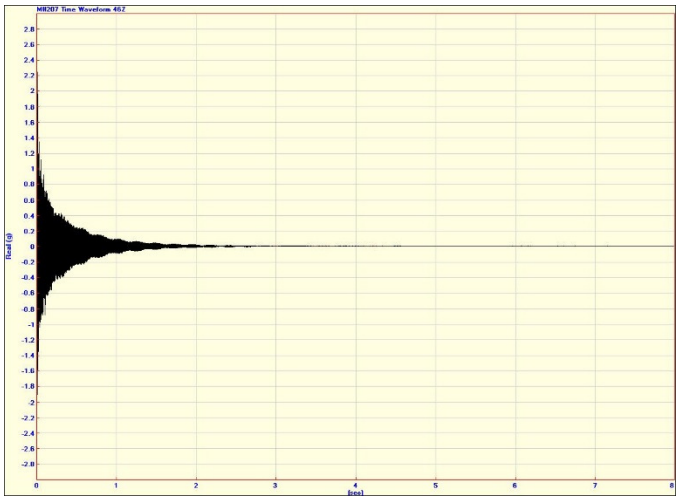

Figure 33. Time waveform of response data.

The auto spectrum of the impulse provides initial information to determine the approximate range of frequencies that are excited by a given hammer tip. The flat region below the first cut-off frequency shows a range in which the hammer applies full force down to a half power of the force. This is denoted by 0.707 $(1/\sqrt{2})$ of the initial amplitude (Balachandran & Magrab, 2008). The auto spectrum shown in Figure 34 indicates the cut-off frequency at 383 Hz.

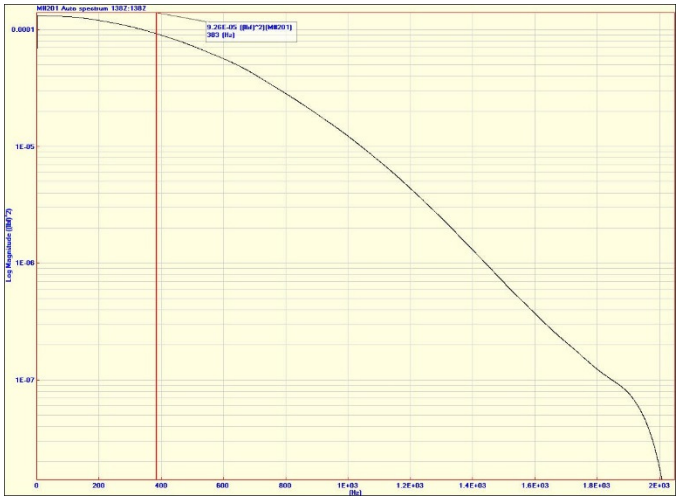

Figure 34. Auto spectrum of impulse showing the cut-off frequency as a red line.

The coherence data shows strength and clarity of data up to 665 Hz as shown in Figure 35. Above 665 Hz there are only discrete ranges with quality data.

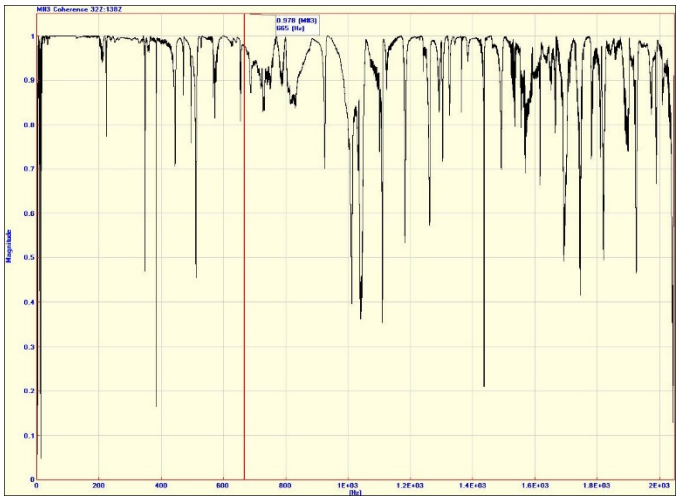

Figure 35. Coherence of measured data at a single DOF.

A coherence value of 1 represents good measurements. At resonance or antiresonance coherence is expected to be low. This can be illustrated by looking at Equation 4 used to calculate coherence (γ^2).

Equation 4

$$\gamma^2 = \frac{H_1(\omega)}{H_2(\omega)}$$

Where

Equation 5

$$H_1(\omega) = \frac{S_{fx}(\omega)}{S_{ff}(\omega)} \quad , H_2(\omega) = \frac{S_{xx}(\omega)}{S_{xf}(\omega)}$$

At resonance the force signal is influenced so $S_{ff}(\omega)$ is vulnerable. Near antiresonance the response is subject to error so $S_{xx}(\omega)$ will suffer. If these quantities suffer the coherence will no longer be unity.

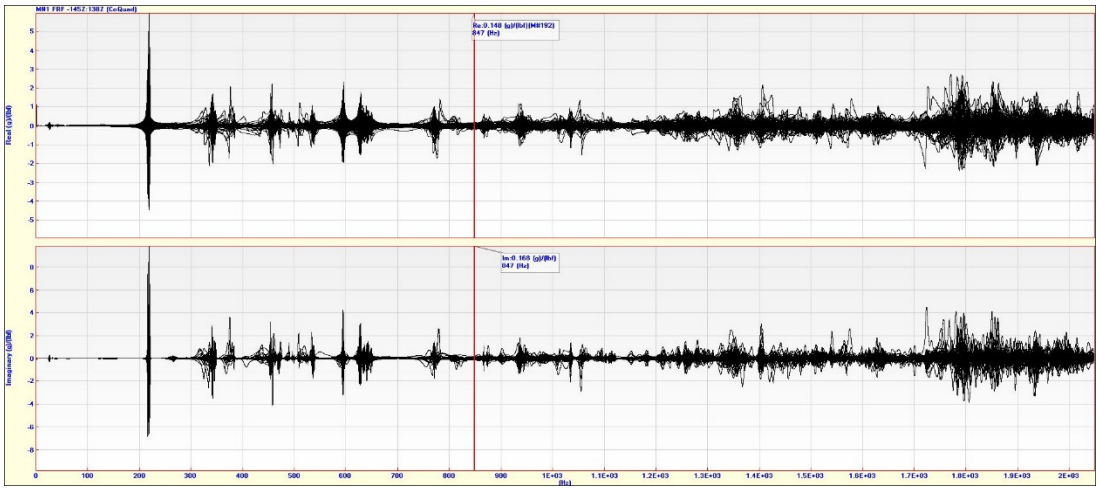

Figure 36. Overlay of all 192 FRF's.

Figure 36 show clarity of the real and imaginary plots with an overlay of FRF's for all DOF's. The signal is good up to 847 Hz then begins to shows signs of degradation. Inspection of the magnitude plot, shown in Figure 37, of the FRF for a single DOF show a discrete frequency range from 345 Hz to 445 Hz where there is some signal noise. Data is not used in this region to draw any conclusions.

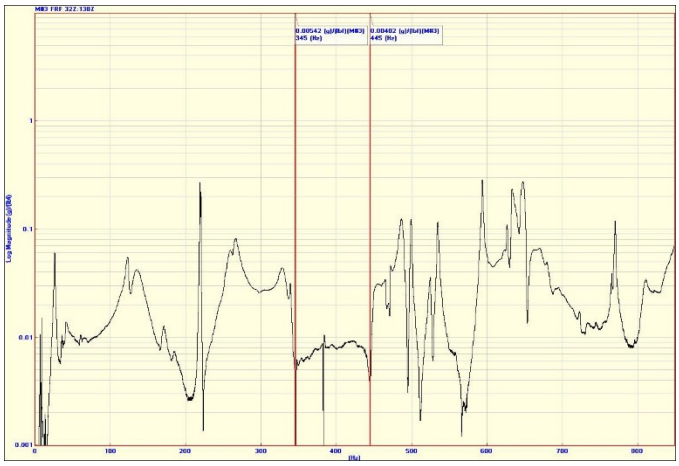

Figure 37. FRF of a single DOF.

Signal fidelity, which ensures the data truly represent the desired quantity, is maintained by ensuring there is not significant motion in the transverse axis of the accelerometer and the mounting was adequate for the desired frequency range. Additionally, channel assignments are checked every time data is collected to verify accurate labeling of data points in the model.

The repeatability of the data is checked by repeating a complete setup and collection of data on 8 measurement points. Table 1 represents the maximum percent change from one setup to the next.

Table 1. Repeatability of measured data.

Mode	Maximum % Change	
	Frequency	Damping
1	0.95 %	52.26%
5	0.16 %	40.22%
6	0.02 %	18.16%

Measurement repeatability of the frequency is within 1% and damping is over 52%. The variation in damping from one collection setup to the next introduces an error in using this parameter for structural health monitoring. After processing of the data, the mounting method

utilized was suspected of introducing changes to the damping of the system. The sensors were mounted with magnetic bases and 8 sensors were applied simultaneously along a single angular line. A test was performed to determine the measurement reliability by changing the test setup to use a single magnetic mounted sensor. The single channel data were then compared to the data from multiple magnetic mounts.

Table 2. Reliability of measured data.

Mode	Maximum % Change	
	Frequency	Damping
1	3.60 %	688.29%
5	1.78 %	152.45%
6	0.67 %	322.09%

Table 2 show the reliability of the data when a different setup was used. The difference in this setup was the use of 1 magnetic mounted sensor compared with 8 magnetic mounted sensors. The use of 8 sensors caused very significant damping changes to the structure. The magnetic sensor mounting method introduces an error in the actual amount of damping in the rotor. In this application the error of the damping measurement exceeds acceptable limits to use it as a useful parameter in this application.

The choice of magnetic mounting was used to apply this in an industrial application. Other mounting methods such as petro wax and adhesive mounting are not as feasible. Petro wax, commonly used in modal testing, requires a clean surface and must not have elevated temperatures to adequately adhere sensors to the surface. An industrial rotor in a glass plant has elevated temperatures and oil on the surface that significantly reduce the effectiveness of petro wax mounting. Adhesives also require clean surfaces and adequate cure time to be effective.

The in-situ conditions therefore would require additional preparation for petro wax and adhesive mounting to be effective. This would increase the collection time significantly making these mounting methods less feasible than magnetic mounting for in-situ testing.

Conclusions

A SHM test is desired which can be implemented in a manufacturing environment to accurately identify compromised rotating components of machines. A feasible in-situ test can be completed quickly during a shutdown opportunity with limited access to components. The use of SHM using modal parameters has been shown in multiple studies to provide an accurate means of identifying structural faults. The goal of this study is to apply SHM and validate such a SHM test procedure for accurately identifying a compromised bolted fastener.

A specific application that would benefit from a SHM test was identified. The test procedure was applied to an industrial fan rotor used in a glass manufacturing plant. The ideal in-situ test utilized minimal collection locations to identify changes in natural frequencies and/or damping. In order to validate the test procedure a full grid collection was performed on a lab setup of the rotor. This identified global modes which could be used for field in-situ testing. The global data results showed significant changes to damping and mode shapes as a result of a removed fastener. Damping changed by as much as 52% for one of the modes and close to 30% for another mode with a fastener removed. These results suggested damping could be used as an indicator for a compromised bolted connection in the rotor. Modal assurance criterion between the as-built rotor and the rotor with a removed fastener also showed significant changes. In one test, 5 of 6 mode shapes significantly changed. Global data results did not show significant changes to natural frequencies of any modes. This indicated natural frequencies were not feasible indicators for the SHM test.

Given the results from the global data a sample of local data points was utilized to represent a feasible in-situ test data set. Local data was reviewed to determine natural frequency and damping changes due to a removed fastener as well as varying fastener torque. Similarly to the global data, results obtained from local data indicated that compromised fasteners did not change the natural frequency of the rotor significantly enough to be used as a structural health monitoring indicator. Local data showed damping was significantly affected by the removal of a fastener, changes in fastener torque, and slight structural modifications. However, review of local data identified significant limitations to the damping results. The deviation in changes from point to point were of similar magnitude as the average change in damping. This error prevents using damping changes as an accurate means of positively identifying a compromised fastener. In addition to significant deviation, no single point or mode provided consistent changes in damping due to structural modifications. Other limitations found in damping changes were related to the mounting method used for attaching accelerometers to the test structure. The magnet mounting used introduced structural changes and was found to cause significant damping changes to the structure.

The lack of changes to natural frequency and the limitations in damping results do not allow this study to produce a simple and quick test procedure for in-situ SHM to be used in a manufacturing environment. Global data did provide accurate information by utilizing modal assurance criterion. Modal assurance criterion could be used for future work to determine the minimum amount of points necessary to monitor changes in mode shapes as a SHM indicator. Future work should also focus on a quick and simple way of mounting the sensors in an industrial application that will not significantly alter the modal parameters.

This study contributes to the field of structural health monitoring by applying it to a real world application and showing the limits and potential for the application. In order to use SHM for this application the fan rotor could be tested prior to being placed in service and then tested at a later date if removed from service. This would allow for adequate collection time to measure the global data needed for mode shape identification. Mode shapes can then be used for MAC to determine if the structure has been compromised. The MAC results could then be used to determine if the fan rotor should be discarded or could be placed back into service at a future date.

Bibliography

Balachandran, B., & Magrab, E. (2008). *Vibrations.* Independence: Cengage Learning, Inc.

Doebling, S. W., Farrar, C. R., Prime, M. B., & Shevitz, D. W. (1996). *Damage identification and health monitoring of structural and mechanical systems from changes in their vibration characteristics: a literature review.* Los Alamos: Los Alamos National Laboratory LA-13070-MS.

Ewins, D. (2000). *Modal Testing theory, practice, and application.* Hertfordshire: Research Studies Press LTD.

Hwang, H., & Kim, C. (2004). Damage detection in structures using a few frequency response measurements. *Journal of Sound and Vibration*, 1 -14.

Karthikeyan, M., & Tiwari, R. (2010). Detection, localization, and sizing of a structural flaw in a beam based on forced response measurements - An experimental investigation. *Mechanism and Machine Theory*, 584-600.

Liu, D., Gurgenci, H., & Veidt, M. (2004). In situ damage detection in frame structures through coupled response measurements. *Mechanical Systems and Signal Processing*, 573-585.

Robert C. Juvinall, K. M. (2000). *Fundamentals of Machine Component Design.* New York: John Wiley & Sons, Inc.

Vibrant Technology, Inc. (2001). *ME'scopeVES Operating Manual.* Jamestown : Vibrant Technology, Inc.

Wolff, T., & Richardson, M. (1989). Fault detection in structures from changes in their modal parameters. *Proceedings of the 7th International Modal Analysis Conference.* Las Vegas: IMAC.

Young, W. C. (1989). *Roark's Formulas for Stress & Strain.* New York: McGraw-Hill, Inc.

Appendix A

The equation of motion for the single degree of freedom (DOF) spring mass system is:

Equation 6

$$m\ddot{x} + c\dot{x} + kx = 0$$

With the natural frequency given by:

Equation 7

$$\omega_n = \sqrt{\frac{k_{eq}}{m_{eq}}}$$

The following schematic illustrates the equivalent spring stiffness for the fan.

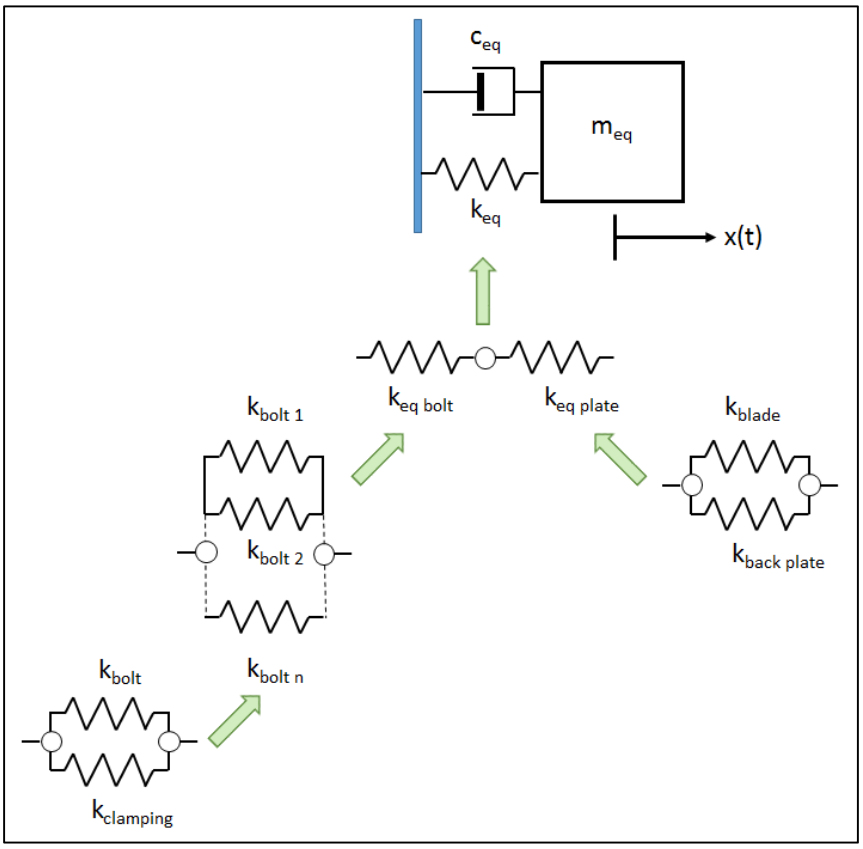

Figure 38. Schematic of single DOF representation of fan rotor with equivalent stiffness of connections.

The following equations show the combination of springs to represent k_{eq}. The equivalent spring stiffness for the single DOF system is defined by springs in series.

Equation 8

$$\frac{1}{k_{eq}} = \frac{1}{k_{eq\ bolt}} + \frac{1}{k_{eq\ plate}}$$

Rearranging this equation to solve for k_{eq} gives the following equation.

Equation 9

$$k_{eq} = \frac{k_{eq\ bolt} \times k_{eq\ plate}}{(k_{eq\ bolt} + k_{eq\ plate})}$$

The equivalent spring stiffness for the plate is defined by springs in parallel.

Equation 10

$$k_{eq\ plate} = k_{blade} + k_{back\ plate}$$

Equation 11

$$k_{blade} = \frac{3 \times E \times I}{l^3}$$

Given:

E = *modulus of elasticity*

$$I = \frac{b \times h^3}{12}$$

$k_{back\ plate}$ is calculated by using Roark's formulas (Young, 1989) for flat circular plates of constant thickness with the outer edge free and the inner edge fixed and the relationship $F = k_{back\ plate} \times y_a$ with unit force applied to the outer edge. Equation 12 is the deflection of a plate at the outer edge given the previous stated boundary conditions and the variables as listed below.

Equation 12

$$y_a = \frac{-w \times a^4}{b \times D} \times \left(\frac{C_2 \times C_9}{C_8} - C_3\right)$$

Given:

$y_a = plate\ deflection\ at\ a$

$a = outer\ radius$

$b = inner\ radius$

$w = force\ per\ unit\ of\ circumferential\ length$

$$D = \frac{E \times t^3}{12 \times (1 - v^2)}$$

$$C_2 = \frac{1}{4} \times \left[1 - \left(\frac{b}{a}\right)^2 \times \left(1 + 2 \times ln\frac{a}{b}\right)\right]$$

$$C_3 = \frac{b}{4 \times a} \times \left[\left[\left(\frac{b}{a}\right)^2 + 1\right] \times ln\frac{a}{b} + \left(\frac{b}{a}\right)^2 - 1\right]$$

$$C_8 = \frac{1}{2} \times \left[1 + v + (1 - v) \times \left(\frac{b}{a}\right)^2\right]$$

$$C_9 = \frac{b}{a} \times \left[\frac{1 + v}{2} \times ln\frac{a}{b} + \frac{1 - v}{4} \times \left[1 - \left(\frac{b}{a}\right)^2\right]\right]$$

$v = Poisson's\ ratio$

$$I = \frac{b \times h^3}{12}$$

The equivalent spring stiffness for the 12 bolted connections is defined by springs in parallel and following equation with n = 12.

Equation 13

$$k_{eq\ bolt} = k_{bolt\ 1} + k_{bolt\ 2} + \cdots + k_{bolt\ n}$$

The spring stiffness provided by each bolted connections is defined by (Robert C. Juvinall, 2000).

Equation 14

$$k_{bolt\ n} = k_{bolt} + k_{clamping}$$

Equation 15

$$k_{bolt} = \frac{A_b \times E_b}{g}$$

Equation 16

$$k_{clamping} = \frac{A_c \times E_c}{g}$$

Given:

A_b = *cross sectional area of bolt*

$A_c = \frac{\pi}{4} \times \left[\left(\frac{d_3+d_2}{2}\right)^2 - d_1^2\right]$

E = modulus of elasticity

g = combined thickness of plates bolted together

d_1 = *bolt diameter for close clearances*

d_2 = *contact diameter for head and nut of bolt*

$$d_3 = d_2 + g \times \tan 30°$$

The equivalent spring stiffness for the plate is defined by springs in parallel for the back plate and blades.

Equation 17

$$k_{eq\ plate} = k_{back\ plate} + k_{blades}$$

Equivalent mass was calculated as from the following equation.

Equation 18

$$m_{eq} = m_{back\ plate} + m_{blades}$$

Appendix B

Instrumentation Specifications

Transducer / Instrument	Model Number	Serial Number	Sensitivity / Specifications
Accelerometer	622A01	10533	100 mV/g, Frequency Response: (±5%) 0.58 to 6000 Hz, Measurement Range: ± 50 g
	622B01	LW43905	98 mV/g, Frequency Response: (±5%) 0.58 to 6000 Hz, Measurement Range: ± 50 g
	622B01	LW43904	98 mV/g, Frequency Response: (±5%) 0.58 to 6000 Hz, Measurement Range: ± 50 g
	622A01	10527	96 mV/g, Frequency Response: (±5%) 0.58 to 6000 Hz, Measurement Range: ± 50 g
	622B01	LW43900	98 mV/g, Frequency Response: (±5%) 0.58 to 6000 Hz, Measurement Range: ± 50 g
	622B01	LW43902	99 mV/g, Frequency Response: (±5%) 0.58 to 6000 Hz, Measurement Range: ± 50 g
	622B01	LW43901	97 mV/g, Frequency Response: (±5%) 0.58 to 6000 Hz, Measurement Range: ± 50 g
	622B01	LW43903	99 mV/g, Frequency Response: (±5%) 0.58 to 6000 Hz, Measurement Range: ± 50 g
IMI Impact Hammer	E086C40	10805	8.69 mV/lbf
NI Data Acquisition Controller	PXI 1033		Express data transfer to laptop
NI Signal Conditioning Module	NI PXI 4472B		102.4 kS/s, ± 10 V, 24 bit A/D, 110 dB dynamic range, AC/DC coupling with IEPE conditioning

Appendix C

MAC Data

		Bolt 10 Removed					
	Mode	1	2	3	4	5	6
AsBuilt	1	0.35	0.04	0.23	0.07	0.05	0.03
	2	0.06	0.59	0.09	0.02	0.00	0.01
	3	0.85	0.09	0.89	0.30	0.01	0.00
	4	0.15	0.07	0.18	0.78	0.06	0.00
	5	0.05	0.01	0.02	0.14	0.68	0.00
	6	0.00	0.00	0.00	0.00	0.01	0.73

Figure 39. MAC data for case #1.

		Bolt 2 Removed					
	Mode	1	2	3	4	5	6
AsBuilt	1	0.98	0.02	0.85	0.12	0.05	0.01
	2	0.06	0.30	0.03	0.03	0.01	0.00
	3	0.90	0.02	0.94	0.17	0.02	0.01
	4	0.17	0.09	0.25	0.80	0.03	0.01
	5	0.01	0.01	0.06	0.00	0.71	0.01
	6	0.00	0.00	0.00	0.01	0.00	0.61

Figure 40. MAC data for case #2.

		Bolt 10 and 2, 40 ft-lb					
	Mode	1	2	3	4	5	6
AsBuilt	1	0.36	0.03	0.28	0.06	0.03	0.03
	2	0.04	0.68	0.05	0.11	0.01	0.01
	3	0.86	0.03	0.94	0.27	0.01	0.00
	4	0.16	0.03	0.22	0.85	0.05	0.00
	5	0.05	0.02	0.01	0.09	0.74	0.00
	6	0.00	0.01	0.00	0.00	0.00	0.48

Figure 41. MAC data for case #3.

		Bolt 2 Removed					
	Mode	1	2	3	4	5	6
Bolt 10 Removed	1	0.96	0.01	0.83	0.11	0.05	0.01
	2	0.16	0.27	0.09	0.07	0.01	0.00
	3	0.84	0.03	0.90	0.14	0.02	0.01
	4	0.16	0.02	0.29	0.54	0.07	0.02
	5	0.00	0.01	0.07	0.00	0.68	0.00
	6	0.01	0.00	0.00	0.01	0.00	0.23

Figure 42. MAC data for case #4.

Local Frequency and Damping Comparison

Mode 1 - Frequency (% Change)					Mode 1 - Damping (% Change)				
DOF	Case #1- As Built vs Bolt 10 Removed	Case #2 - Bolt 10 and 2, 40 ft-lb vs Bolt 2 Removed	Case #3 - As Built vs Bolt 10 and 2, 40 ft-lb	Case #4 - Bolt 10 Removed vs Bolt 2 Removed	DOF	Case #1- As Built vs Bolt 10 Removed	Case #2 - Bolt 10 and 2, 40 ft-lb vs Bolt 2 Removed	Case #3 - As Built vs Bolt 10 and 2, 40 ft-lb	Case #4 - Bolt 10 Removed vs Bolt 2 Removed
7Z	0.3%	0.0%	0.4%	0.7%	7Z	39.8%	13.3%	40.1%	12.2%
21Z	1.0%				21Z	1.9%			
32Z	2.4%	0.0%	3.2%	0.9%	32Z	24.0%	10.2%	27.0%	12.8%
36Z	1.9%	0.2%	3.1%	1.0%	36Z	2.6%	70.3%	5.9%	46.1%
60Z	0.2%	0.0%	1.2%	1.3%	60Z	43.9%	14.5%	13.4%	31.2%
101Z	1.9%	0.4%	3.4%	1.2%	101Z	9.2%	36.6%	30.6%	0.2%
151Z	2.3%	0.0%	3.1%	0.8%	151Z	19.3%	20.8%	43.3%	11.3%
161Z	0.6%	0.0%	0.2%	0.8%	161Z	9.5%	21.6%	24.4%	12.0%
Average	1.3%	0.1%	2.1%	1.0%	Average	18.8%	26.8%	26.4%	18.0%
Std Dev	0.8%	0.1%	1.3%	0.2%	Std Dev	15.1%	19.5%	12.5%	14.3%

Figure 43. Frequency and damping % change for mode 1.

Mode 5 - Frequency (% Change)						Mode 5 - Damping (% Change)				
DOF	Case #1- As Built vs Bolt 10 Removed	Case #2 - Bolt 10 and 2, 40 ft-lb vs Bolt 2 Removed	Case #3 - As Built vs Bolt 10 and 2, 40 ft-lb	Case #4 - Bolt 10 Removed vs Bolt 2 Removed	DOF	Case #1- As Built vs Bolt 10 Removed	Case #2 - Bolt 10 and 2, 40 ft-lb vs Bolt 2 Removed	Case #3 - As Built vs Bolt 10 and 2, 40 ft-lb	Case #4 - Bolt 10 Removed vs Bolt 2 Removed
7Z	0.9%	0.5%	0.0%	1.4%	7Z	42.7%	18.6%	8.3%	59.5%
21Z	2.7%				21Z	17.6%			
32Z	1.4%	0.0%	0.1%	1.5%	32Z	15.9%	3.3%	23.1%	51.3%
36Z	3.4%	0.3%	1.1%	2.0%	36Z	46.4%	45.9%	46.8%	83.5%
60Z	0.3%	0.1%	1.6%	1.2%	60Z	18.9%	9.6%	75.7%	63.4%
101Z	3.1%	0.3%	1.6%	1.1%	101Z	29.6%	17.4%	11.2%	91.1%
151Z	1.6%	0.1%	0.0%	1.5%	151Z	23.6%	2.8%	11.9%	50.7%
161Z	1.1%	0.3%	0.7%	1.4%	161Z	38.3%	14.7%	11.7%	67.8%
Average	1.8%	0.2%	0.7%	1.4%	Average	29.1%	16.0%	27.0%	66.7%
Std Dev	1.0%	0.2%	0.7%	0.2%	Std Dev	11.2%	13.5%	23.4%	14.3%

Figure 44. Frequency and damping % change for mode 5.

Mode 6 - Frequency (% Change)						Mode 6 - Damping (% Change)				
DOF	Case #1- As Built vs Bolt 10 Removed	Case #2 - Bolt 10 and 2, 40 ft-lb vs Bolt 2 Removed	Case #3 - As Built vs Bolt 10 and 2, 40 ft-lb	Case #4 - Bolt 10 Removed vs Bolt 2 Removed	DOF	Case #1- As Built vs Bolt 10 Removed	Case #2 - Bolt 10 and 2, 40 ft-lb vs Bolt 2 Removed	Case #3 - As Built vs Bolt 10 and 2, 40 ft-lb	Case #4 - Bolt 10 Removed vs Bolt 2 Removed
7Z	0.1%	0.2%	0.1%	0.1%	7Z	11.8%	19.7%	55.5%	119.7%
21Z	0.1%				21Z	38.6%			
32Z	0.1%	0.2%	0.1%	0.1%	32Z	9.4%	7.0%	116.4%	112.5%
36Z	0.1%	0.2%	0.1%	0.1%	36Z	10.0%	1.6%	141.8%	123.4%
60Z	0.6%	0.2%	0.6%	0.1%	60Z	80.7%	0.2%	58.2%	117.0%
101Z	0.2%	0.2%	0.2%	0.1%	101Z	45.2%	1.6%	216.8%	121.8%
151Z	0.1%	0.2%	0.1%	0.1%	151Z	8.2%	0.6%	143.1%	163.4%
161Z	0.1%	0.2%	0.1%	0.1%	161Z	12.1%	10.4%	69.5%	115.5%
Average	0.2%	0.2%	0.2%	0.1%	Average	27.0%	5.9%	114.5%	124.7%
Std Dev	0.2%	0.0%	0.2%	0.0%	Std Dev	24.4%	6.7%	54.4%	16.1%

Figure 45. Frequency and damping % change for mode 6.